UPPER MANTLE VELOCITY STRUCTURE IN EASTERN KANSAS FROM TELESEISMIC P-WAVE RESIDUALS

by

Roger K. Hahn
B.A., Emporia State University, 1975

Submitted to the Department of Geology and the Faculty of the Graduate School of the University of Kansas in partial fulfillment of the requirements for the degree of Master of Science.

[1980]

Professor in Charge

Committee Members

For the Department

ABSTRACT

The Kansas Geological Survey (KGS) has been operating a telemetered microearthquake seismograph network in Eastern Kansas since July, 1977. The nine stations in the array are spaced about 80 kilometers (km) apart and the distance across the array is roughly 200 km. The Midcontinent Geophysical Anomaly (MGA), which is believed to be an expression of a late Precambrian rifting episode, lies in the western third of the array. Teleseismic P-wave residuals have been calculated for 37 events that occurred from December, 1978, to May, 1980. These residuals have been corrected for recording filter, elevation, and sedimentary section thickness differences. Relative residuals are azimuthally dependent at four of the stations, although few azimuths are represented. Because the KGS array has been designed for recording microearthquakes rather than teleseisms, the quantity and quality of teleseismic data has suffered somewhat. Nevertheless, these data indicate the presence of a low-velocity body in the upper mantle beneath the MGA. Whereas the western extent of the low-velocity material cannot be ascertained with the present network, the easternmost limit appears to be between 150 and 200 km east of the rift axis. Assuming an arbitrary, but reasonable, five percent velocity decrease, the anomalous material is constrained to the upper 100 km of the mantle. Because the rifting ceased about 1.1 billion years ago and there is no present-day evidence of high heat flow from the MGA, the low-velocity body is attributed to residual compositional differences related to differentiation of magma in the upper mantle.

TABLE OF CONTENTS

LIST OF ILLUSTRATIONS

LIST OF TABLES

ACKNOWLEDGEMENTS

Special thanks go out to my advisor, Don Steeples, for his guidance and encouragement. In addition to my other committee members, George Rothe and Bob Miller, I would like to thank the staff of the KGS. Max Coe, John Oldfather, and Nancy Prohaska provided invaluable assistance with computer matters. Pat Acker and Bruce Bandle helped with the preparation of the illustrations. Rex Buchanan read the manuscript; thanks for the suggestions. Others on the KGS staff, too numerous to mention, gave their help and support throughout.

Sherri Peroli helped with the typing, but more importantly, provided moral support and understanding, thank you!

INTRODUCTION

The teleseismic P-wave delay method is a powerful tool that enables seismologists to investigate the crust and upper mantle beneath an array of seismograph stations. Variations in travel times of P-waves from teleseisms or distant explosions recorded over an array of stations can be reduced to station delay times. Since the waves emerge at 15 to 30 degrees from vertical, the delay times can be interpreted in terms of the velocity-depth function in the crust and upper mantle in the vicinity of the array.

The Kansas Geological Survey (KGS) has been operating a microearthquake seismograph array in Eastern Kansas since July, 1977. In the spring of 1978 the seismograph array was enlarged from the original six to the present nine stations. In January, 1979, a digital tape recording system was installed. The equipment additions resulted in a substantial increase in both the quantity and the quality of teleseismic data available for study.

The objective of this thesis is to use the teleseismic data available to conduct a P-wave delay study of Eastern Kansas. Because a large part of the data are of insufficient quality, care must be taken to systematically select the most reliable information. Teleseismic arrival times are reduced to delay times and this information is used to construct a geologic model that best explains the observed perturbations in P-wave travel times.

THE TELESEISMIC P-WAVE DELAY METHOD

Gutenberg (1953) first inplied the use of teleseismic P-wave delays when he made a statement on his study of P-wave travel times from the Kern County, California, earthquake of 1952:

> The errors of the average travel-time curves for direct longitudinal waves are now probably smaller than the effects of the local structure near the source and the station. The corresponding differences in travel times depend mainly on the depth of the Mohorovicic discontinuity at the source (in shallow earthquakes) and the station, and may amount to 3 seconds or even more at distances of a few degrees and at least 2 seconds at greater distances.

Depth to the Moho is probably not the chief factor responsible for variable delay times at sources and stations (Cleary and Hales, 1966). Nevertheless, two important points must be considered. First, in order to obtain greater precision, the source and station effects must be separated from the average travel times (that is, relative delays rather than absolute delays are used). Second, to achieve such separation, either the variation of these effects with distance must be taken into account, or the analysis should be confined to a distance range within which variation is negligible. The preferred distance range (from the seismograph array to the epicenter) has been shown to be from 40 to 100 degrees of great-circle distance (Barr and Robson, 1963; Bolt and Nuttli,1966).

For epicentral distances of less than 30 to 40 degrees, the amplitudes of P-waves are reduced and timing the onset of the waveform becomes more difficult. Events closer than 20 degrees are not truly teleseisms and should be considered as a separate and distinct data set. As the distance surpasses 100 degrees, the shadow zone of direct P-wave arrivals is encountered.

Not only is the distance range important, but the directions from the seismograph array to the events is of great importance. Several distinctly different azimuths are required if a P-delay study is to reveal a dipping interface or a horizontal velocity variation (Nuttli and Bolt, 1969).

In standard convention, residuals (i.e. delays) are defined as the difference between the observed arrival time (t_o) and the arrival time predicted by a standard empirical travel-time table such as the Herrin (1968) table (t_H). By this definition, the residual (r_H^i) at the i^{th} station is:

$$r_H^i = t_o^i - t_H^i \tag{1}$$

The residual found from the above expression is called the absolute residual and is of little value for P-delay studies. Absolute residuals are nothing more than a measure of the inaccuracies in the computed hypocenter and origin time of the event, and the deviation the true P-wave velocity from the Herrin (1968) earth P-velocity . Hence, for local P-delay studies, relative residuals are cal- d to nullify these errors. Relative residuals are obtained by e station as a reference and then subtracting the absolute

residual at the reference station (r_H) from absolute residuals at the other stations. For example, if the I^{th} station is used as the reference, the relative residual (R_H^i) at the i^{th} station will be:

$$R_H^i = r_H^i - r_H^I \tag{2}$$

If R_H^i is positive, a delay must have occurred somewhere along the ray path from the earthquake hypocenter to the i^{th} station relative to the ray path to the reference station. Conversely, if R_H^i is negative, a decrease in travel time (i.e. an increase in velocity) must have occurred somewhere along the ray path to the i^{th} station relative to the ray path to the reference station. As the focus of the event represents essentially a point source, the rays to different stations of a small array follow very similar paths until they are far from the focus. Because the lower mantle is thought to be homogeneous on a scale of several kilometers (Hart, 1969), it is reasonable to assume that most of the contribution to the relative residuals of an array comes from crustal or upper mantle velocity differences beneath the array. The possibility of source effects on the relative residuals still exists. However, as a general rule source effects introduce uncertainties of less than 0.1 second (sec) into the data (Engdahl et. al., 1977).

The selection of a reference station may be somewhat arbitrary, although two criteria should be met. First, the reference station should be reliable so that as many events as possible are recorded (that is, the reference station chosen should be the one most likely to record any given event). Secondly, the reference station should

be situated near the area of the suspected anomaly, but far enough away so that ray paths from events to the station are not affected by the anomalous body regardless of the location of the event. If the reference station selected is situated near an anomalous area, then interpretation may be more difficult. In such a case the ray paths from one direction to the reference station would encounter the anomalous body while ray paths from another direction would pass through more or less of the anomalous body, or miss it entirely. As a result, the relative residuals may depend not only upon the geologic structure beneath the array, but also upon the selection of the reference station. The result could be an incorrect interpretation of the residual data, although by exercising great care in the analysis such problems can be avoided.

The resolving power of a seismograph array for a P-delay study is governed by the station spacing, the number of stations, and the diameter of the array. The maximum depth of exploration is approximately the diameter of the array, whereas the lateral resolution is about equal to the average station spacing. Features shallower than the station spacing are sparsely sampled so that the resolution down to that depth is poor except directly under the individual stations.

As an example of the physical meaning of P-wave residuals, consider the effect of a low-velocity body on the relative residuals. Figure 1 shows the relative positions of a low-velocity body, the seismograph stations, and ray paths for events from the east and the west. The P-wave velocity decreases in the low-velocity material and this segment of the ray path is darkened. In this case, station E

would be the ideal choice for the reference station because ray paths from both directions are not influenced by the anomalous body. For events approaching from the east, stations A, B, and C will have positive relative residuals. For events approaching from the west, stations C and D will have positive relative residuals. The magnitude of the residual will be proportional to the length of the ray path within the low-velocity material and the velocity difference between the two media.

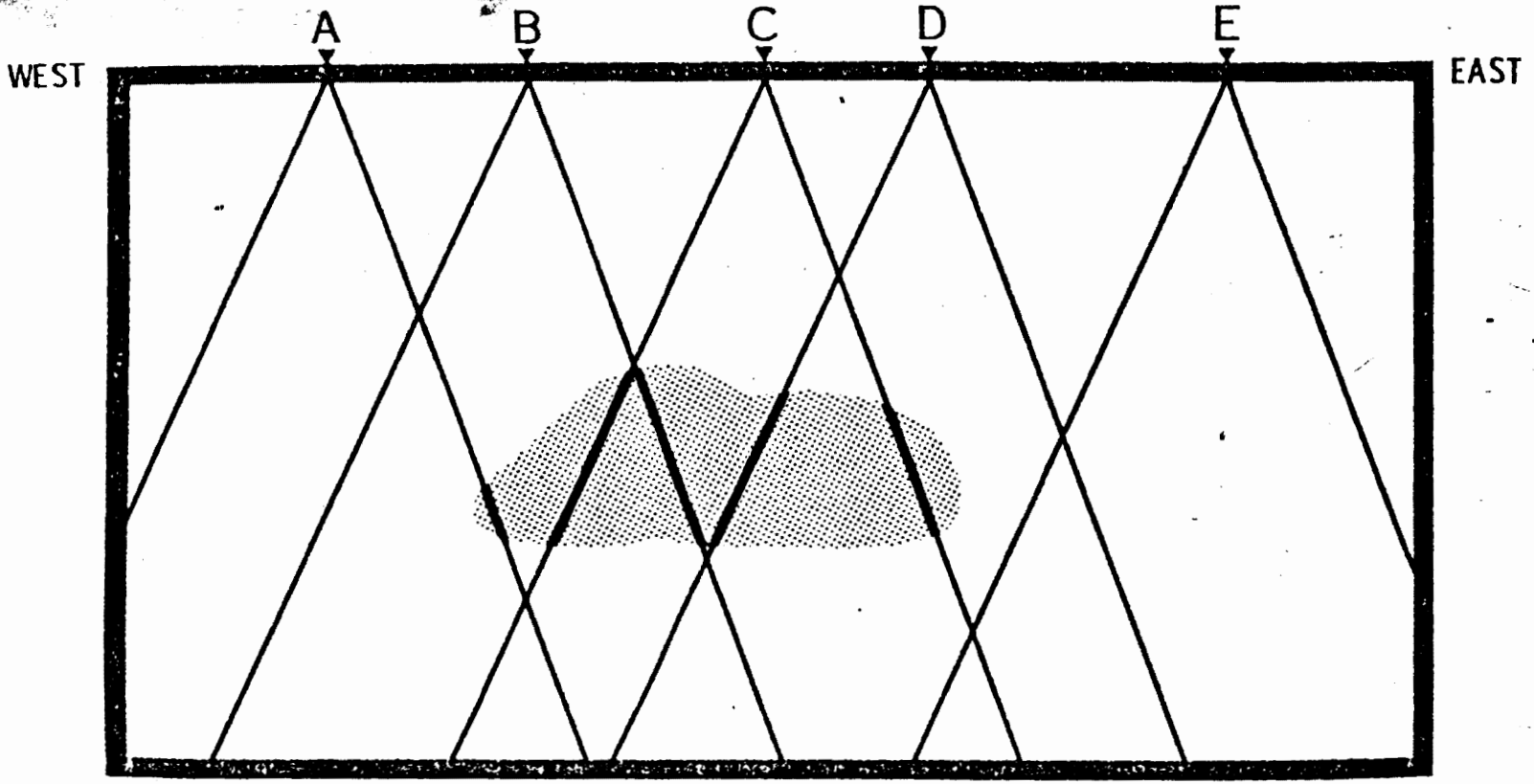

FIG. 1. A schematic representation of the ray paths from two teleseisms (one from the east; the other from the west) to seismograph stations A, B, C, D, and E. The darkened segments correspond to a velocity decrease while propagating through lower-velocity material.

PREVIOUS INVESTIGATIONS

The teleseismic P-wave delay method has become widely used in crustal and upper mantle velocity studies. Barr and Robson (1963) supplemented gravity data with P-wave data in an effort to derive a crustal cross section from the Venezuelan Basin eastward into the Atlantic Ocean. Talwani and Sutton (1963) criticized the method of Barr and Robson's gravity reductions but stated that, "this (seismic delay method) is a very useful added parameter to the solution of the crustal structure problem."

Press and Biehler (1964) also used correlations between P-wave delays and gravity anomalies to infer crustal structure. They hypothesized higher than normal temperatures in the lower crust beneath the Sierra Nevada batholith, but an alternate interpretation of their data may be possible in view of later work involving azimuthal variation in P-delays. Bolt and Nuttli (1966) and Nuttli and Bolt (1969) investigated relative P-delays in Northern California. They found azimuthal variations of up to 2.4 sec and suggested that these effects were due to changes in the depth or thickness of the low-velocity layer in the upper mantle. Bolt and Nuttli (1966) commented on the work of Press and Biehler (1964), saying that the delays they reported may occur only for the azimuth of 275°. Press and Biehler (1964) used events with 270° to 280° azimuths exclusively and this matter cannot be settled without obtaining P-delay information on events from other directions.

More recently, P-delays have been used to study the velocity structure in geothermal areas. Iyer (1975) and Evans and Iyer (1975) have shown P-delays of up to 2 sec at Yellowstone. These delays have been attributed to a low-velocity material that extends from within the crust down to at least 250 km depth and possibly to 400 km or more. This is the first geothermal area studied by the P-delay technique, and the results may have important implications for the mantle plume hypothesis (Steeples and Iyer, 1976a). Steeples (1975) and Steeples and Iyer (1976a,b) subsequently used the P-delay technique to infer the presence of anomalously hot rock in the crust beneath Long Valley caldera and at The Geyesers geothermal area in California.

Local seismic refraction and reflection surveys provide information that is essential to the interpretation of P-delays. Such local studies supply near surface velocity information that is needed in order to remove the near surface effects and concentrate on deeper structure. Warren and Healy (1973) used the latest interpretations of refraction data to compile a contour map of the Mohorovicic discontinuity for the conterminous United States. They indicate a crustal thickness of 42 km at St. Joseph, Missouri, and 51 km in Southeast Kansas. Steeples (1976) presented a preliminary interpretation of a 500 km refraction profile from Concordia, Kansas to Agate, Colorado. The crust thickens from 38 km at Concordia to 48 km at Agate, assuming that the crustal velocity persists at 6.1 km/sec down to the Moho.

THE SEISMOGRAPH ARRAY

The Geographic Setting

Figure 2 shows the locations of KGS seismograph stations in Eastern Kansas. Typical station spacing is about 60 to 80 km and the total distance across the array is roughly 200 to 220 km. Because of the size and spacing of the array, a P-delay study using the KGS network will be limited to fairly large scale features located primarily in the upper mantle.

Kansas is a rather poor geographic location for a teleseismic P-delay study because of the distance and direction to many of the world's seismic areas. Alaska, South America, Central America, and Mexico are the only major areas of seismicity that are relavant to a P-delay study in Kansas. The seismically active western portion of the Circum-Pacific Belt lies beyond the 104 degree range of direct P-arrivals (i.e. the shadow zone). To the east, the only source of activity is the Mid-Atlantic Ridge, since the Trans-Eurasian Belt (Iran and Turkey for example) is also in the shadow zone. Unfortunately earthquakes at mid-ocean ridges are shallow and usually small. Such events are poor sources of P-delay information because their energy is rapidly attenuated and consequently sharp P-arrivals are rare.

Deeper events usually provide better quality P-arrivals because the focus is below the often complex crustal and upper mantle structures encountered in seismically active regions. Alaskan earthquakes are typically shallow, but not necessarily small. Only the larger Alaskan events are generally acceptable and, therefore, only a fraction of the total number of Alaskan events can be used. Mexican and Central American events are only 20 to 25 degrees distant from Kansas and at such short distances the errors can easily be equal to or greater than the measured delays. Fortunately, many South American events are deep and of sufficient magnitude to produce sharp P-wave arrivals. In addition, most of the South American events lie beyond 40 degrees.

Description of the Study Area

Kansas is located in the continental interior, a place that has been popularly thought of as representing normal crust. A deep seismic reflection survey in Eastern Kansas is currently being undertaken by the Consortium for Continental Reflection Profiling (COCORP). One reason COCORP is involved in Kansas is that the planners wanted to gather data from what they considered to be normal crust.

However, the crust in Kansas is not as normal as it was commonly thought to be 20 or 30 years ago. A striking feature on gravity and magnetic maps of Kansas is the Midcontinent Geophysical Anomaly (MGA). The MGA extends from Lake Superior to Kansas and perhaps into Oklahoma (Coons, Woollard, and Hershey, 1967) and consists of four en echelon narrow positive gravity belts with flanking lows. Geologic

investigations in the northern segments have shown a clear association of the MGA with rocks of Keweenawan age (about 1.1 billion years). In the near surface, basic lavas and gabbros correlate with the positive feature, and sandstones and shales with the flanking lows (Ocola and Meyer, 1973).

Ocola and Meyer (1973) compared the geophysical and geological characteristics of the MGA with those of seven well known rifts and ridges. They found an extraordinary match between the MGA and the known rifts and concluded that the MGA should be properly classified as a rift. They subsequently adopted the highly interpretive name, Central North American Rift System (CNARS).

The interpretation of the MGA as a rift structure is not new. For example, in 1916, Martin inferred a rift structure in the Lake Superior region from geologic data (Ocola and Meyer, 1973). Today, the MGA is widely accepted as being the result of a continental rifting episode about 1.1 billion years ago (Chase and Gilmer, 1973; Ocola and Meyer, 1973).

Figure 2 shows the approximate location of the MGA in Kansas (as located by King and Zietz, 1971) and the KGS seismograph locations. Figure 3 is a Bouguer gravity map of Northeast Kansas (compiled by Yarger, et. al., 1980) with the locations of all but the two southernmost KGS seismograph stations. Yarger (1980) derived a crustal cross section across the MGA from magnetic and gravity data. Figure 4 shows this cross section along with the measured and computed gravity and magnetic proviles (the line of section, A-A', is shown on Figure 3). Yarger's profile passes almost directly over the

station CNK and about 30 km north of TCK; the positions of these stations are shown on Figure 4.

East of the MGA lies the Nemaha Ridge and Humboldt fault zone, a major structural feature in Eastern Kansas. This feature trends generally north to south and approximately parallels the MGA. The vertical displacement on the Humboldt reaches nearly 4000 feet in Northeast Kansas (Ward, 1974) and the fault zone passes within 10 km of the stations EDK and BEK (Cole, 1976).

Cole (1976) compiled a contour map of the top of the Precambrian rocks in Kansas from well information. This map was used to estimate the depth to the Precambrian rocks under each seismograph station, whereas United States Geological Survey (USGS) 7.5 minute quadrangle maps were used to find the elevation, latitude, and longitude of each station. Table 1 gives the location, and Precambrian and surface elevations for each station.

strumentation

The instruments used in the KGS seismograph array were selected for recording microearthquakes in Kansas, not for recording distant earthquakes. The frequency content of the energy from the two types of events is different. Microearthquakes are high-frequency (5-15 Hz) events and the instruments are adjusted to pass this energy while attenuating the lower-frequency (1 Hz) teleseismic energy. As a result, the amplitudes of teleseisms will be reduced, depending upon the filter and gain characteristics of the individual station.

The seismometers used in the KGS seismograph network are Teledyne Geotech' S-500's. These seismometers use the piezoelectric properties of the quartz crystal rather than the standard magnet-and-coil arrangement. The S-500 geophone is a short-period accelerometer of extreme sensitivity. Velocity output is obtained from an operational amplifier contained within the seismometer. The seismometers are installed at the bottom of 190 foot bore holes to cancel high frequency cultural and wind noise.

The signal from the seismometer is filtered and amplified by a Sprengnether AS-110 amplifier. A voltage controlled oscillator (VCO) then converts the signal to a frequency modulated (FM) signal before sending the information to the KGS building in Lawrence, Kansas, via long-distance telephone circuitry. The FM signal is then converted back to analog voltage information and recorded. All the stations, except BEK, have been telemetered in the above manner since the installation of the array.

Prior to August 1, 1979, the recorder for BEK was operated by a volunteer who checked the time, changed the paper, and mailed the seismograms in to the KGS. This procedure resulted in considerable timing uncertainties, as it was impossible to synchronize the clock at BEK with those located at the KGS. On August 1, 1979, telemetry from BEK to the KGS building was established and BEK has since been recorded at the KGS along with the other stations.

The signals telemetered from the field to the KGS are recorded on nine Teledyne Geotech RV-320 Portacorder ink-and-paper chart recorders. The Portacorders further amplify and filter the informa-

tion. Each Portacorder contains a quartz crystal clock for keeping time for that particular recorder.

The clocks are synchronized to each other and to the WWV radio broadcast of Universal Coordinated Time (UCT) daily. Because each Portacorder contains its own clock rather than using a single clock for all nine Portacorders, some timing error is introduced. To ensure accurate relative times, synchronization marks are put on the records daily. The marks go on all nine records simultaneously so that the records can be synchronized to each other to within .02 sec, even though the absolute time for the whole network may be off by as much as 0.1 sec. The fact that the absolute time may be off is of no consequence in this study because it deals with relative rather than with absolute residuals.

As stated above, the seismic information is filtered and amplified both in the field and in the office. The filters and gains are adjusted to maximize the signal-to-noise ratio for each station. Because teleseismic energy is typically 1 Hz, the selection of a high-cut filter is irrelevant. However, the low-cut filters will reduce the amplitudes of the teleseismic data. Low-cut filters in the field are either out or set at 5 Hz, whereas the low-cut filters on the Portacorders are either 5 Hz or 10 Hz. Filter and gain settings are not constant for any one station, but rather they are changed occasionally in response to seasonally variable station noise characteristics. Nevertheless, each station can be characterized by a normal or typical combination of filters and gains. The effect of

filters on timing is discussed below. Table 2 gives normal filter and gain settings for each station.

The Digital Recording System

In addition to the paper-and-ink chart recorders, a digital tape recording system has recorded some of the teleseisms. An Input/Output Inc., DHR 1632 seismic exploration system has been modified to provide a digital recording medium. The modifications are done on a single read-only-memory circuit board that can be interchanged in seconds to convert the system from an eight-channel exploration seismograph to an eight-station digital earthquake recording system. Memory capacity of the system (16 K) allows for eight stations to be recorded at 31.25 samples per second for 64 sec. Either 10 or 24 sec of pre-event data are recorded in order to ensure the recording of the first P-arrival. When the memory is full, data are automatically put on tape and the system returns to the listen mode. The event detection condition is that all three stations within a trigger group show increased activity within a given time period of roughly 28 sec.

There are several advantages to using the digital tape records. Data on digital tape can be subjected to computer techniques such as cross-correlation of waveforms for increased timing accuracy. Data can also be filtered to bring out the 1 Hz energy of teleseisms while attenuating the higher frequency signal and noise. The gain can be changed from station to station in order to amplify the signal at those stations with poor records. The digital records also have more

low frequency content than the paper records because the signal bypasses the low-cut filters in the Portacorders. The greatest advantage of digital over analog data for this study is that the relative time on the digital records is exact because the data from all stations go onto the tape simultaneously.

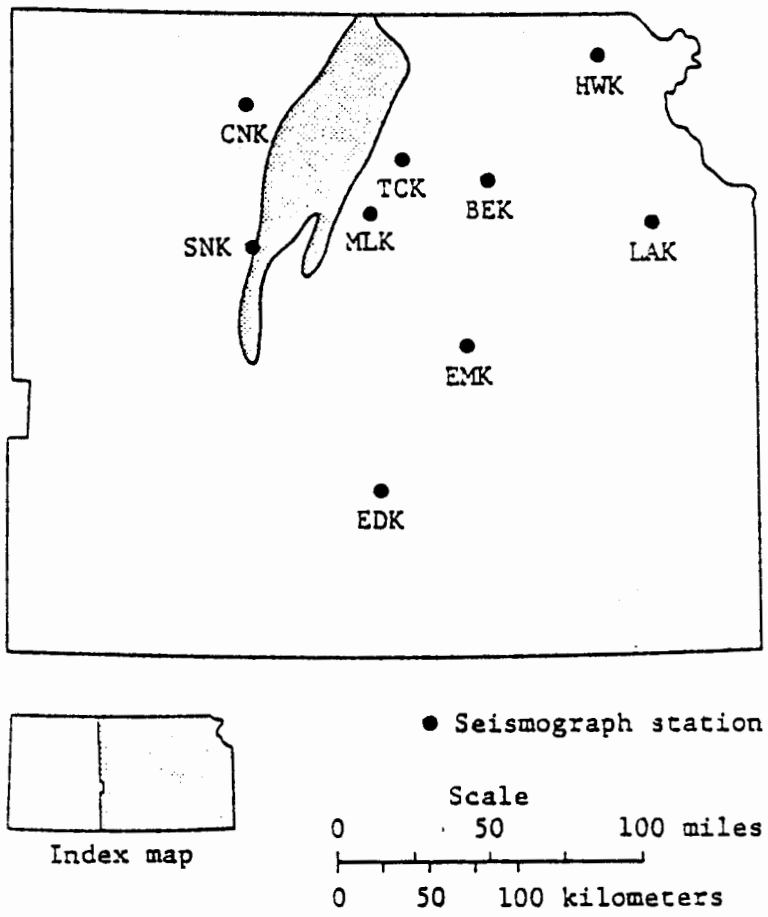

FIG. 2. Location of the KGS seismograph stations. The Midcontinent Geophysical Anomaly (MGA), as located by King and Zietz (1971) is shaded.

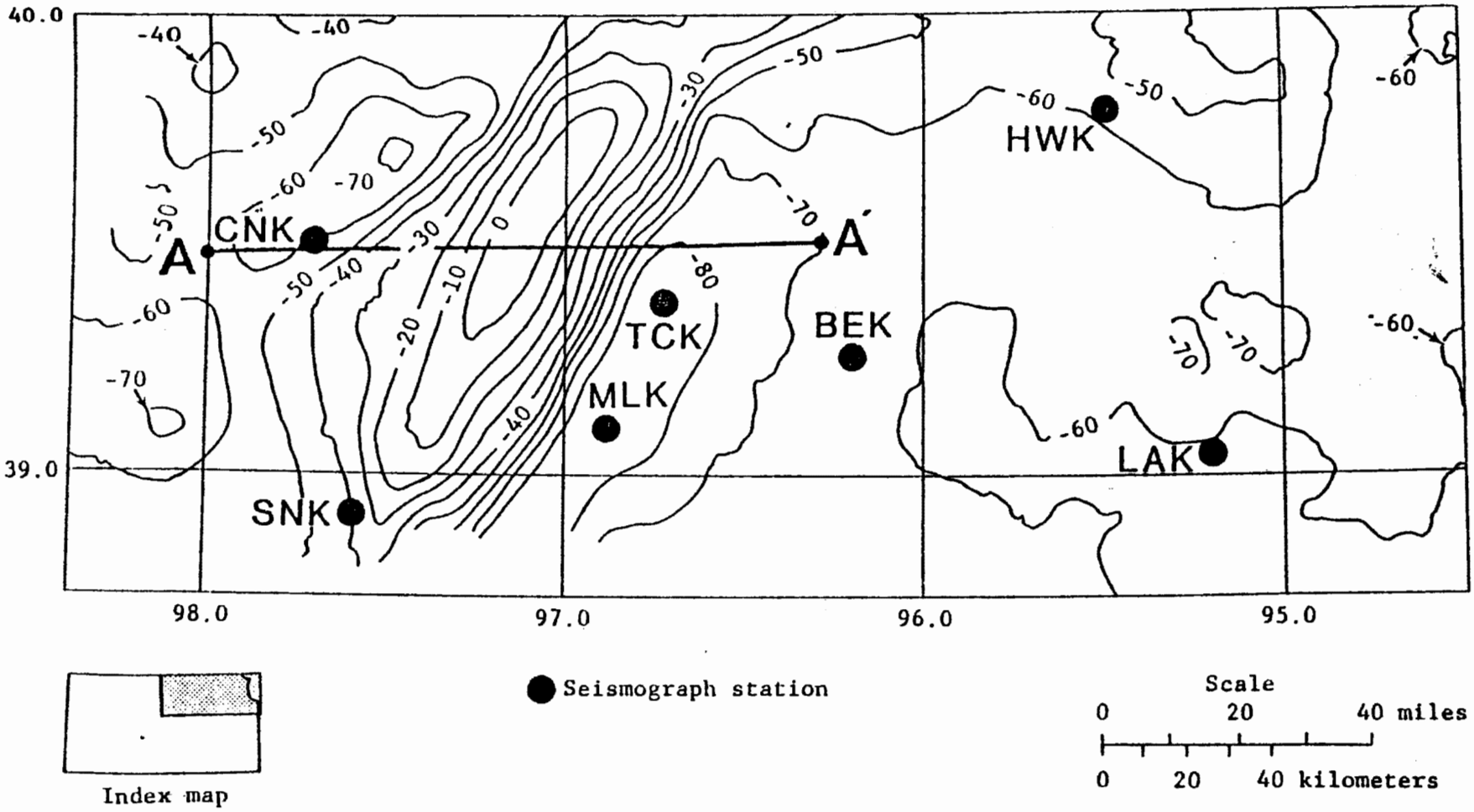

FIG. 3. Bouguer gravity map of northeast Kansas. Line A-A' is the line of section shown on Fig. 4 (after Yarger, et al., 1980).

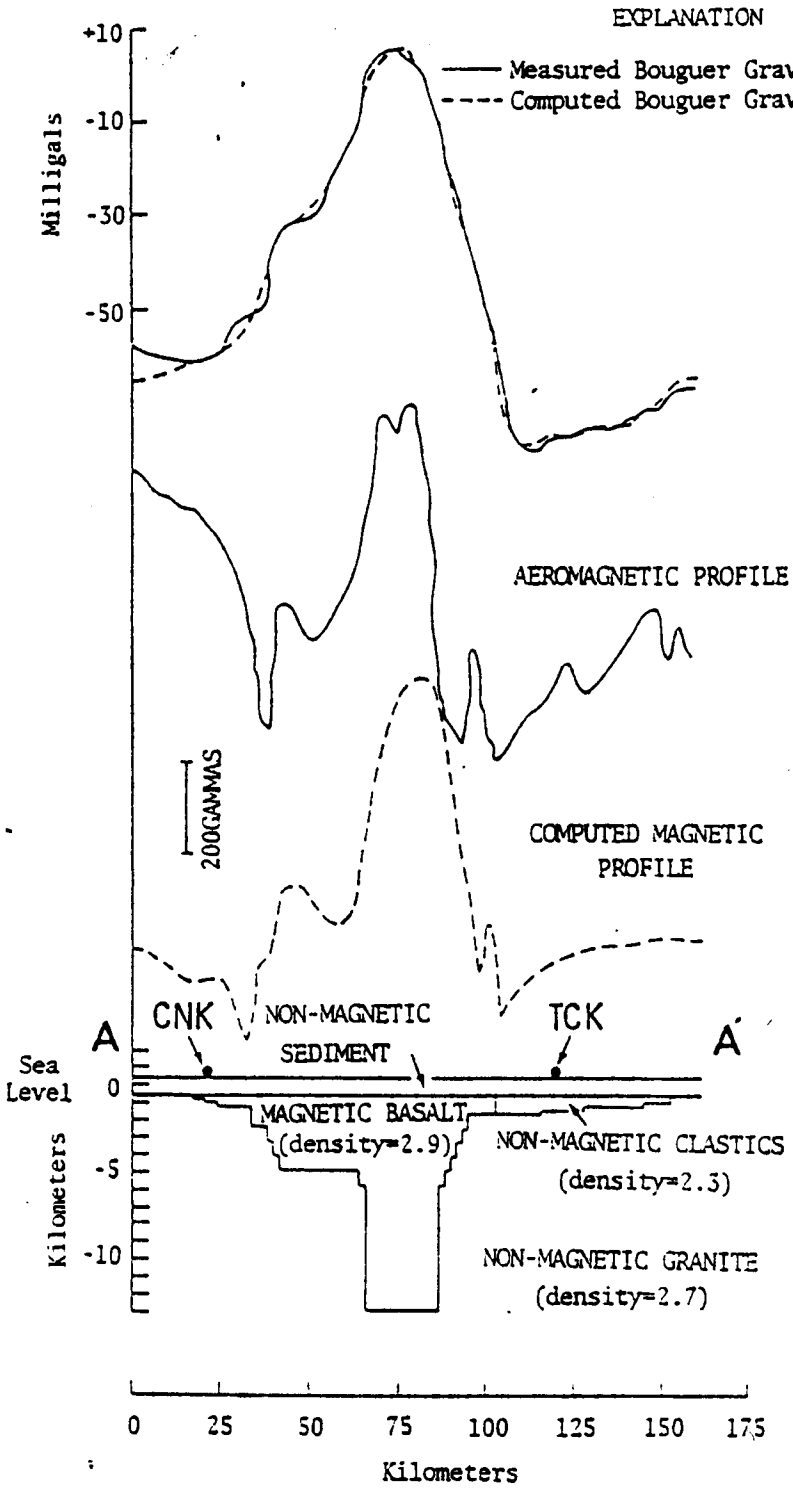

FIG. 4. Crustal cross-section derived from east-west magnetic and gravity profiles across the MGA from 96.15° to 98.0° W. longitude at 39.5° N. latitude. Magnetic parameter values for basalt favored by computer model are: remnant inclination = +70°, remnant declination = -70°, and susceptibility = 0.0004. Line A-A' is shown on Fig. 3. (After Yarger, 1980)

TABLE 1. STATION LOCATIONS

STATION	NORTH LATITUDE		WEST LONGITUDE		ELEVATION (m)	PRECAMBRIAN-SURFACE ELEVATION (m)
	deg	min	deg	min		
LAK	39	2.78	95	12.27	326	-533
HWK	39	48.13	95	29.79	320	-802
BEK	39	15.79	96	11.98	349	-671
EMK	38	26.79	96	19.03	307	-664
EDK	37	46.43	96	47.70	418	-802
MLK	39	6.36	96	53.54	386	-503
TCK	39	23.09	96	43.35	377	-396
SNK	38	57.18	97	36.18	407	-832
CNK	39	30.48	97	42.78	465	-771

TABLE 2. STATION FILTER AND GAIN INFORMATION

STATION	FIELD AMPLIFIER		RECORDER AMPLIFIER	
	Low-Cut Filter (Hz)	Gain (dB)	Low-Cut Filter (Hz)	Gain (dB)
LAK	5	96	10	72
HWK	0	78	5	72
BEK	5	90	5	78
EMK	0	84	10	78
EDK	5	90	10	72
MLK	0	84	10	72
TCK	0	84	5	72
SNK	5	84	5	78
CNK	0	90	5	72

OBSERVATIONAL MATERIAL

At the beginning of this study all teleseismic data collected at the KGS were examined and their overall quality was judged. Ideally only data from the distance range of 40 to 100 degrees are used. However, a significant portion of the available data were from events closer than 40 degrees. Therefore, to expand the data set events in the range 20 to 40 degrees were included. Unfortunately, a limited number of distinct azimuths are represented, due to the geographical relationship of the KGS network to the areas of seismicity. For best results, only events for which sharp, impulsive first arrivals are recorded at all or virtually all of the stations should be used (Cleary and Hales, 1966), but this requirement is impossible to meet in this study. Therefore, events were chosen for study if TCK (chosen as the reference station) and at least two other stations recorded sharp first arrivals. For any given event, anywhere from three to nine stations could be used in calculation of residuals.

The final, and most important criterion to be met in the selection of events was time accuracy. For any given event, if the arrival time at all stations could be considered accurate to within 0.1 sec, then that arrival was used for calculating residuals. This 0.1 sec time standard takes into account the synchronization of the individual clocks as well as picking the same phase of the P-wave arrival . The location, date, origin time, depth to focus, and arrival times for the events used are listed in Appendix A.

METHOD OF DATA REDUCTION AND ANALYSIS

Timing P-Wave Arrivals

Because this investigation is concerned with relative rather than absolute residuals, it is more important to pick the same phase of the P-wave at all stations than to pick the earliest arrival. Figure 5 shows some representative seismograms and various picking conventions. Several investigators at the USGS have adopted the practice of picking the zero crossing rather than the first break of the P-wave energy (Steeples and Iyer, 1976a). For poorly recorded teleseisms resulting from small events or background noise, the first break, the first peak or trough, and the first zero crossing are often obscured in such a way that the second zero crossing is the first and most reliable pick. Reading beyond the second zero crossing introduces intolerable levels of uncertainty due to reflections, scattering, diffraction, and other wave deformation phenomena (Mack, 1969). For this study, the second-zero-crossing method was used where possible. Where this was not feasible the first break or first zero crossing was used.

All timing of the paper records was done visually. However, the digital records were picked both by visual inspection and by use of a cross-correlation computer program described by Reasenberg (1978) and modified by Coe (1980). Coe's version uses the sign bit only, which

means that frequency is the determining factor. Because the amplitudes often vary considerably from station to station, Coe's program often was more useful than Reasenberg's.

Computer picking is accomplished by making a pick on a reference trace (usually, but not necessarily TCK) and then letting the computer find where that pick has the best mathematical fit with the other traces. The output of the program tells how many samples each trace must be delayed or advanced in order to get the best fit with the reference trace. As the sample rate is known to be 31.25 samples per second, the time offset can be calculated to within 1/31.25 or .032 sec at best.

A visual check of the computer pick was always made before the pick was accepted. Often the visual pick and computer pick agreed to the exact sample point. In other instances the computer found a waveform that was obviously off by several seconds, yet showed the best fit to the reference pick. In such cases the correlation function was examined. The correlation coefficient of the visual pick was generally only slightly less than the coefficient of the computer pick. Because the computer pick was obviously wrong and the visual pick correlated nicely to the reference, the visual pick was used to calculate the residual.

Calculation of Residuals

Other than the location and arrival time for each receiving station, the only information required to calculate residuals is the hypocenter location and the origin time of the earthquake.

Hypocenter and origin time information are found in the monthly listings of the Preliminary Determination of Epicenters (PDE). The PDE is published by the National Earthquake Information Service with funding from the United States Department of the Interior via the USGS.

Before the relative residuals can be calculated, a reference station must be selected. Because TCK had a history of providing the best teleseismic records, it was chosen as the reference station. Not only has TCK recorded the most teleseismic events, it also gives the clearest, most easily timed P-wave arrivals.

The actual calculation of the relative residuals was performed by computer. The program used, DISTAZRES, was compiled by several researchers at the USGS in Menlo Park, California. Hypocenter location and origin time, plus arrival times and station locations are the input. The output from the program consists of : (1) The great-circle distance from each station to the epicenter in degrees (DELTA); (2) the direction from each station to the epicenter along a great circle in degrees from north (AZIMUTH); (3) the theoretical travel time to each station as given by the Herrin (1968) tables; (4) the absolute residual for each station; (5) the reciprocal of the apparent velocity in degrees (DT/DDEL); (6) the direction from the epicenter to each station (BACK AZIMUTH); and (7) relative residuals using up to five different reference stations.

The procedure outlined above would be complete only if all the seismograph stations were at the same elevation and were undelain by the same sedimentary section. Obviously this is not the case and

corrections must be made at each station for the near surface effects on the P-wave arrival times. Making the corrections is rather arbitrary. For example, all stations could be reduced to sea level with the Precambrian surface continued upward to sea level, but this would require considerable manipulation of arrival times.

The best way to make station corrections is to minimize the amount of rock that must be added or subtracted in order to make all stations equal. From Table 1 station EMK is located at the lowest surface elevation and SNK is situated above the lowest Precambrian-surface elevation relative to the other stations. It was decided to lower the surface elevation of each station to that at EMK (307 m) and to lower the Precambrian-surface elevation at each station to that at SNK (-832 m). This procedure requires two corrections: (1) removal of rock above 307 m elevation, and (2) replacement of granite above -832 m with sedimentary rock.

The time (t_s) required for the P-wave to travel through the removed surface material is given by equation (3) and the additional time (t_g) required as a result of replacing granite with sedimentary rock is given by equation (4).

(3) $$t_s = (z_s/v_s)\text{Cos}X$$

(4) $$t_g = z_g(1/v_s - 1/v_g)\text{Cos}X$$

Where:

X = angle the emerging ray makes with vertical,

z_s = thickness of the removed surface material,

v_s = velocity of the P-wave in the sedimentary section,

z_g = thickness of granite replaced with sedimentary rock,

v_g = velocity of the P-wave in the granite.

For this investigation X was set at 20°; v_s and v_g were assigned values of 3.4 km/sec and 6.0 km/sec, respectively. The value selected for X represents a good approximation for events from Alaska and South America, the most important events in terms of the analysis of the residual data. The values selected for the velocities come from local seismic exploration studies carried out by the KGS and the USGS (Steeples, 1976).

The total station correction (T) is found by simply subtracting t_s from t_g. Due to the relatively short distances and good velocity information, T can probably be considered accurate to within .02 sec. As T is dependent upon the geologic setting of each station and can therefore be regarded as constant, it is added to the observed arrival time of each station in a subroutine in DISTAZRES before the calculation of residuals. Table 3 lists the station corrections.

The final point to consider in calculating residuals is the effect of filtering the seismic signal. Because the passband varies somewhat from station to station, it was necessary to find out what difference, if any, the filters might make in the relative P-wave arrival times. Two experiments were performed to observe the time

delay effect of the field amplifier and the Portacorder filter on 1 Hz seismic waves.

First, the effect of the low-cut field filters was observed. A 1 Hz signal from a function generator was sent through a field amplifier and to one trace of a dual trace oscilloscope. The same signal was also passed directly from the function generator to the other trace of the oscilloscope. With the low-cut filter out, the two waveforms coincided. Next, the 5 Hz low-cut filter was applied while observing the oscilloscope. Even though the wave amplitude was affected by the filter, the zero crossing of the filtered wave still coincided with that of the unfiltered wave. The experiment was repeated with the 10 Hz low-cut filter and the results were the same. Because the zero crossing is generally used to time the P-wave arrivals, the field filters can be ignored in this study.

A different approach was taken to observe the effect of the Portacorder's low-cut filter on teleseismic data. The function generator was connected directly to the input of a Portacorder and a 1 Hz signal was applied. With the low-cut filter set at 5 Hz, the 1 Hz wave was recorded on paper for several seconds before switching from the 5 Hz to the 10 Hz low-cut filter.

The result was a 1 Hz sine wave with a sizeable amplitude drop where the 10 Hz filter was applied. By measuring the period of several cycles of the wave train and then measuring several cycles from before to after the point where the 10 Hz filter was applied, it was determined that the signal was delayed by .05 sec or less. Because TCK has a 5 Hz low-cut filter, the relative arrival times at

the other stations with the 5 Hz filter need not be adjusted. However, for those stations with a 10 Hz low-cut filter .05 sec was subtracted from the relative residuals. This .05 sec correction was applied to the residuals at MLK, LAK, EDK, and EMK after the residuals were calculated by DISTAZRES as the filters, unlike the geologic setting, can vary somewhat.

Correlation of Residuals with Epicenter Location

Appendix B gives the relative residuals at each station for each event. The events have been grouped according to the source region: South America, Central America, Mexico, and Alaska. These data show considerable scatter in some cases, probably a result of the combination of poor quality data and complex structure beneath the receivers. Because of this scatter, for each group in Appendix B with five or more events, the largest and smallest residuals were discarded before calculating the average and standard deviation. Omitting the largest and smallest residuals has a negligible affect on the mean, but this practice does serve to reduce the standard deviations to values which better represent the accuracy of this study.

Tables 4-7 give the means and standard deviations calculated above. The residuals relative to TCK are plotted on station location maps in Figures 6-9. A 0^{*} plotted next to a station location indicates that the magnitude of the residual is small (less than 0.1 sec) and the standard deviation is equal to or greater than the magnitude of the residual. The 0^{*} can be interpreted as being essen-

tially a zero delay. 'Numbers in parentheses are residuals calculated from only one event and are highly suspect. Numbers followed by an apostrophe indicate a large standard deviation (but less than the signal) and these values are also suspect. In the final anaylsis the residuals corresponding to a 0^*, parentheses, and to an apostrophe are weighted less than the other residuals.

To check for azimuthal variations of the residuals relative to TCK (RR_{TCK}), they were plotted against the azimuths (AZ) (Figure 10). The graphs for EMK, EDK, CNK, and SNK show two linear trends, one for azimuths from 140° to 200° and one for azimuths from 280° to 325°. The straight lines on Figure 10 are least-squares fits to the points. The equations of these lines and the value R^2, a statistical measure of goodness of fit ($R^2 = 1.0$ for a perfect fit), are given in Table 8.

Bolt and Nuttli (1966) and Nuttlii and Bolt (1969) noticed a sinusoidal relationship between P-residuals and azimuth. Figures 10a-10d hint at such a relationship; whereas Figures 10g and 10h show no azimuthal dependence. Figures 10e and 10f appear to suggest sinusoids although too few data are available to be sure. To investigate this sinusoidal relationship, a non-linear regression was performed by computer to fit a simple cyclic curve to the data (Health Services Computing Facility, 1979). The residual function was estimated for each station by fitting, in the least-squares sense, the values of RR_i to the form:

(5) $$RR_i(AZ) = A_i + B_i \, Sin(AZ + E_i)$$

where A_i, B_i, and E_i are constants of the i^{th} station. The values obtained for A, B, and E for each station are listed in Table 9. Figure 11 shows the RR_{TCK} vs. AZ graphs, with the calculated sine curves, for stations EMK, EDK, CNK, and SNK. There are not enough data available for BEK and LAK to meaningfully fit a sine wave to the data. For HWK and MLK, a straight line fits the data almost as well as a sine wave and, therefore, these plots are not presented.

Use of the Average as a Reference

It was also decided to try the average as a reference. Station HWK is the second most reliable to use as a reference, but it experienced electronic problems that resulted in fewer and more weakly recorded teleseisms. Due to intolerable levels of noise at the other stations, the only remaining alternative is the average travel time of the array. Rather than subtracting the absolute residual of the reference station from that at the other stations, the mean of all the absolute residuals can be subtracted from the absolute residual for each station. Each station is then referenced to the average travel time of the array rather than to the travel time for a specific reference station.

This method has been used sparingly (Barr and Robson, 1963) for good reasons. A timing error or picking error at one or two stations will influence the mean and give inconsistant results. Also, poor quality data are weighted the same as good quality data in calculating the mean. Another problem arises when different groups of

stations are used for different events. When this happens, the mean can drift from one event to another. The consequence can be a lack of consistency in the calculated residuals.

Despite the shortcomings of referencing to the average, it was performed. Appendix B gives the residuals for each station relative to the average travel time (RR_{mean}). The residuals are grouped according to the general geographic location of the epicenters and the means and standard deviations of these groups are given in Tables 4-7. The large standard deviations are most likely a result of the inaccuracies in the average method discussed above. The residuals referenced to the mean are plotted against the azimuth in Figure 12. No azimuthal dependence is apparent from these graphs and lines were not fitted to these data. Due to the excessive scatter, uncertainty, and inconclusive nature of these data, the average method was viewed as being fruitless and subsequently abandoned.

Analysis of the Residuals

The sinusoidal nature of the RR_{TCK} vs. AZ graphs (see Figure 10) suggests a non-uniform velocity structure in Eastern Kansas. Nuttli and Bolt (1969) report that differences in either crustal thickness or in crustal velocity relative to the reference station will contribute to the A term in equation 5 (see Table 9). However, one or more dipping interfaces or horizontal velocity variations are required to produce an azimuthal dependence.

Inspection of Table 9 reveals a similarity of the residual functions at EDK, EMK, SNK, and CNK, whereas the residual functions at the other stations appear to be unrelated. This similarity led to the working hypothesis that something in the vicinity of these four stations was responsible for the observed P-residuals. Because the MGA exists in this area, it seems reasonable to investigate the possible connection between the MGA and the observed residuals.

Mueller and Landisman (1966) report evidence of low-velocity zones in the upper 10 km of the crust. Lidiak (1978) cites crustal low-velocity layers as being common among active continental rifts, as a result of a hot crust. However, due to the absence of high heat flow within the MGA and the magnitude of the observed residuals, a crustal cause of the residuals can be rejected on the grounds that this would be inconsistent with the seismic refraction profile presented by Steeples (1976).

The upper mantle appears to be a more logical place to look for a cause of the residuals. In order to formulate a preliminary model, vectors were drawn from the seismograph stations to the three principle epicenter localities: South America, Mexico, and Alaska (Figures 13-15). The vectors are projections of the ray paths to the stations on the surface of the earth. The cross marks on the vectors correspond to points in the subsurface; each cross mark represents 50 km of depth. The head of a vector represents the point on the surface of the earth that is directly above the point in the subsurface, at a depth of 250 km, that is sampled by the seismic ray path.

Comparison of Figures 2 and 6-8 with Figures 13-15 led to the observation that a low-velocity body in the upper mantle in the area of the MGA could largely explain the observed P-residuals. Manual, rather than computerized, ray tracing was then performed in an effort to determine the size and shape of the anomalous body. Ray tracing is a technique often used in interpreting the data from seismic exploration methods. Seismic ray paths from well spaced seismic sources to receivers are used to constrain the size and shape of the anomalous body, depending upon the residuals calculated for the receiving stations (see Figure 1).

To model a subsurface body with the ray tracing technique, it is important to have data from opposite directions (that is, the azimuths of the two sets of data should differ by 180°). By using the events from opposite directions, a two-dimensional model can be generated. If two or more sets of such opposite events are available, a three-dimensional model can be constructed. The accuracy of the model increases with the number of sets of opposite events. Fortunately, the events from Alaska and South America differ in azimuth by about 170°, making these events almost ideal for two-dimensional ray tracing. It is also fortunate that the Alaskan and South American events are generally the most well recorded in the data set. However, as these events represent the only pair of events available for ray tracing, a three-dimensional model would be highly speculative.

Line A-A' on Figure 16 shows the line along which ray tracing was performed. The locations of the seismograph stations are projected onto line A-A' by moving the stations either north or south rather than perpendicularly to A-A'. In this manner, the stations are moved parallel to the general trend of the MGA, preserving the relative positions of the MGA and the seismograph stations. If the stations were projected perpendicularly onto line A-A', then SNK would appear to be on the wrong side of the MGA, next to TCK and MLK rather than CNK. Also, EDK would appear to be the farthest removed from the roughly north-south axis of the MGA.

Figure 17 was prepared to show the relationship between the observed P-delay and the apparent thickness of anomalous material sampled for various percentage velocity decreases. An arbitrary, but reasonable, five percent velocity decrease was chosen in modeling the anomalous body. The five percent velocity decrease was chosen for two reasons. First, a ten percent or greater velocity decrease is thought to require a partial melt (Murase and McBirney, 1973) and there is no evidence of high heat flow from the MGA. Secondly, a two percent velocity decrease would require longer ray paths through the anomalous material than can be justified with ray tracing.

Once the velocity contrast was selected, the areal extent and total thickness of the low-velocity body could be constrained. Inspection of Tables 4-7 reveal that the residuals, relative to both TCK and the mean, for HWK and LAK are consistently negative. Furthermore, these residuals are generally quite large in magnitude. This trend can also be seen on the RR vs. AZ graphs (see Figures 10f,

10g, 12a, 12c). These negative residuals imply that the low-velocity material is either thin or nonexistent beneath HWK and LAK. Unfortunately, there are no seismograph stations located far enough west of the MGA to set a limit on the westward extent of the anomalous material. The magnitudes of the observed residuals limit the apparent thickness of the low-velocity material to about 80 km, assuming a five percent velocity decrease. Figure 18 is a cross section of the crust and upper mantle along A-A'. Projected station locations and ray paths for events from Alaska and South America are shown, as is the model that best fits the residuals.

This model was generated within the limits outlined above. For a starting point, it was assumed that the ray path from Alaska to TCK encountered 80 km of low-velocity material. Next, the thickness of anomalous material sampled by each of the remaining stations was calculated from the observed residuals using a hand calculator and Figure 17. In a trial-and-error process, the thickness, lateral extent, and depth of low-velocity material were adjusted so that the model shown in Figure 18 best fits the observed residuals.

Because the line A-A' on Figure 16 intersects the MGA (see Figure 2) at an oblique angle, the resulting model shown in Figure 18 is somewhat distorted. For this reason a crustal and upper mantle section along line B-B' (Figure 16) was constructed to show the model as it would appear when viewed at right angles to the trend of the MGA (Figure 19). Again, the station locations have been projected north and south onto the line of section. The conversion from Figure 18 to Figure 19 was accomplished using simple trigonometric relation-

ships. The north-south extent of the low-velocity body is poorly constrained. The residuals calculated from Mexican events indicate that the anomalous body is thickest to the south of TCK and becomes quite thin (20 to 40 km thick) to the south of EDK (see Figures 8 and 14).

As is the case with any experiment involving physical measurements, some uncertainty is to be expected in this study. The timing of the P-wave arrivals can generally be considered accurate to within 0.1 sec. As errors in the earth model, hypocenter location, and origin time are nearly nullified by using relative residuals, this 0.1 sec can be considered to be the major source of error. However, the combination of station corrections and crustal complexities can account for an additional 0.05 sec, giving a total maximum uncertainty of 0.15 sec which is equivalent to about 25 km of anomalous material (see Figure 17).

The model presented in Figure 18 was generated using the data from Alaska, South America, and to a much lesser extent, Mexico. A total of 23 ray paths were considered when modeling the anomalous body and the final model fits the data, within the expected uncertainties, in all but four of these cases. For events from Alaska, CNK and EDK do not fit and for events from South America, EMK and LAK do no fit. The data for CNK and LAK probably do not fit because they are of poor quality; the data for EDK and EMK are of much better quality. Because EDK is projected almost 150 km north onto line A-A' on Figure 16, the misfit at EDK could be explained by a thickening of the low-velocity material to the south. A thickening of the anomaly

to the south would contradict the Mexico data, but because Mexico is only 20° from the array, the residuals calculated for Mexican events are suspect and thus weighted less than the residuals found from Alaskan and South American events. The data for EMK imply a rapid 70 km thickening to the southeast of EMK. However, due to the sparse sampling in this area this situation can not be verified with the present network. The failure of EDK and EMK to fit the model is probably a result of structure in Southern Kansas that cannot be resolved with the present KGS seismograph network.

As an alternative to the model proposed in Figures 18 and 19, an attempt was made to explain the residuals in terms of undulations in a mantle low-velocity layer. Green and Hales (1968) analyzed the data from project Early Rise and observed that any low-velocity layer beneath the central United States is either very thin or at a depth of more than 150 km. The ray-tracing technique was used to try to model a low-velocity layer at 150 km depth. At this depth it is impossible to derive a model that will satisfy both the Alaska and the South America data simultaneously. When the low-velocity layer is moved to the upper 100 km of the mantle, the model starts to fit. However, manipulation of the shape of the low-velocity layer to fit the data results in a model that resembles Figure 19, not the modern concept of the low-velocity layer. On these grounds, undulations in the mantle low-velocity layer were discarded as an explanation.

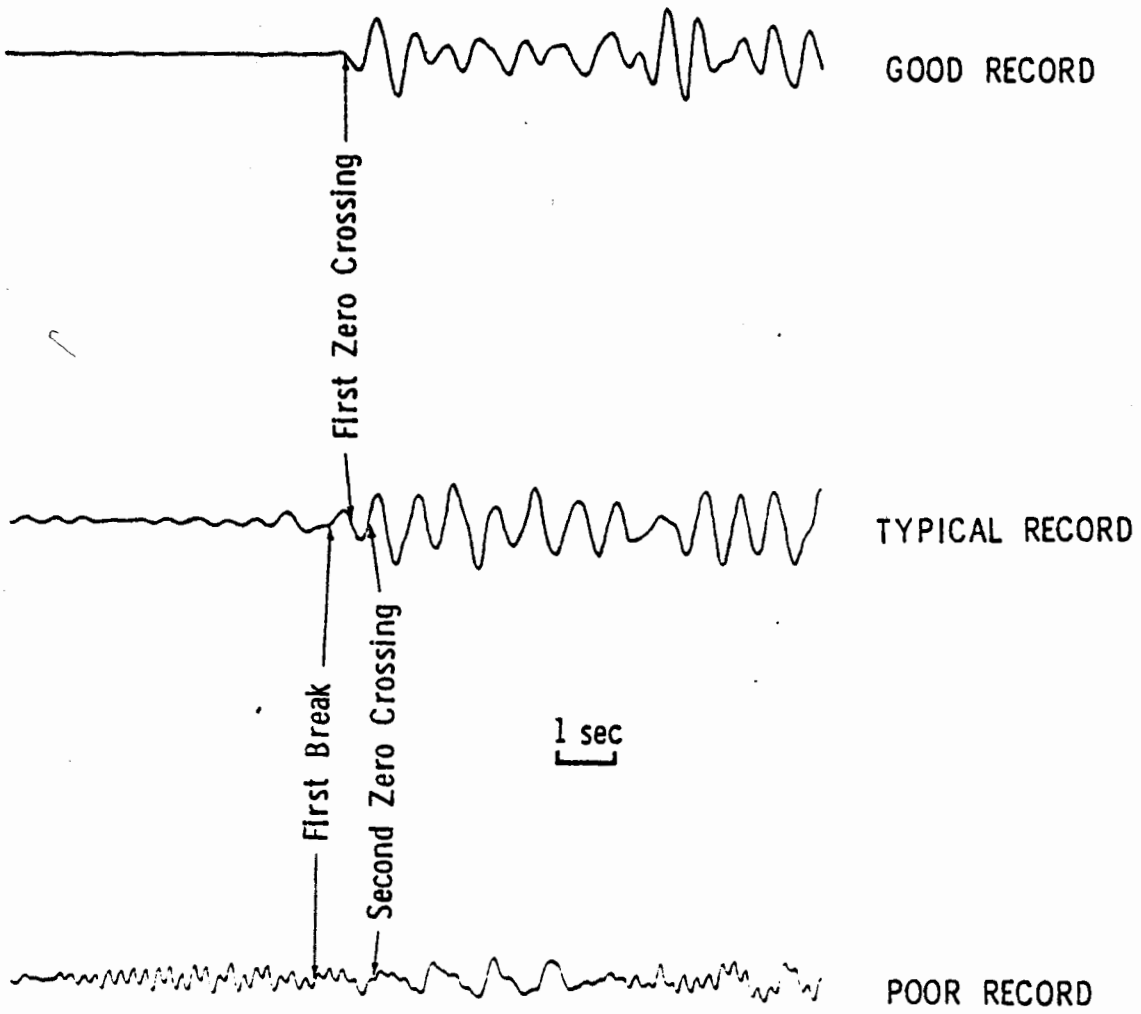

FIG. 5. Representative seismograms illustrating various picking conventions.

TABLE 3. STATION CORRECTIONS

STATION	t_s (sec)	t_g (sec)	T (sec)	FILTER CORRECTION (sec)	TOTAL (sec)
LAK	.005	.036	.03	-.05	-.02
HWK	.004	.004	.00	.00	.00
BEK	.012	.019	.01	.00	.01
EMK	.000	.020	.02	-.05	-.03
EDK	.031	.004	-.03	-.05	-.08
MLK	.022	.040	.02	-.05	-.03
TCK	.019	.053	.03	.00	.03
SNK	.028	.000	-.03	.00	-.03
CNK	.044	.007	-.04	.00	-.04

TABLE 4. SUMMARY OF RESIDUALS FOR SOUTH AMERICAN EVENTS

STATION	NUMBER OF OBSERVATIONS	RESIDUALS RELATIVE TO TCK (sec)		RESIDUALS RELATIVE TO THE MEAN (sec)	
		$\bar{x}$	s.d.	$\bar{x}$	s.d.
LAK	3	-.12	.03	-.14	.02
EDK	2	.08	.07	.05	.05
BEK	1	.04	----	.01	----
CNK	4	.34	.07	.21	.06
SNK	4	.32	.18	.26	.17
EMK	3	.35	.05	.30	.04
MLK	5	-.01	.02	-.03	.01
HWK	3	-.46	.10	-.51	.11
TCK	6	----	----	-.08	.06

TABLE 5. SUMMARY OF RESIDUALS FOR CENTRAL AMERICAN EVENTS

STATION	NUMBER OF OBSERVATIONS	RESIDUALS RELATIVE TO TCK (sec)		RESIDUALS RELATIVE TO THE MEAN (sec)	
		$\bar{x}$	s.d.	$\bar{x}$	s.d.
LAK	1	-.29	----	-.10	----
EDK	0	----	----	----	----
BEK	3	-.07	.03	.11	.01
CNK	1	.72	----	.64	----
SNK	1	.17	----	.09	----
EMK	2	.25	.53	.18	.24
MLK	3	-.33	.01	.10	.06
HWK	3	-.52	.12	-.39	.23
TCK	4	----	----	.09	.12

TABLE 6. SUMMARY OF RESIDUALS FOR MEXICAN EVENTS

STATION	NUMBER OF OBSERVATIONS	RESIDUALS RELATIVE TO TCK (sec)		RESIDUALS RELATIVE TO THE MEAN (sec)	
		$\bar{x}$	s.d.	$\bar{x}$	s.d.
LAK	2	-.56	.32	-.20	.26
EDK	2	-.52	.09	-.18	.01
BEK	3	-.35	.27	-.16	.22
CNK	4	-.34	.07	-.03	.10
SNK	3	-.17	.01	.23	.15
EMK	9	-.40	.14	-.09	.13
MLK	4	-.13	.04	.07	.13
HWK	7	-.41	.18	-.17	.19
TCK	10	----	----	.23	.12

TABLE 7. SUMMARY OF RESIDUALS FOR ALASKAN EVENTS

STATION	NUMBER OF OBSERVATIONS	RESIDUALS RELATIVE TO TCK (sec)		RESIDUALS RELATIVE TO THE MEAN (sec)	
		$\bar{x}$	s.d.	$\bar{x}$	s.d.
LAK	2	-.46	.17	-.20	.06
EDK	3	.26	.03	.25	.34
BEK	0	----	----	----	----
CNK	3	-.07	.10	.04	.04
SNK	6	-.32	.15	-.03	.25
EMK	4	-.31	.18	-.13	.08
MLK	6	.07	.06	.18	.04
HWK	8	-.35	.12	-.25	.10
TCK	8	----	----	.11	.11

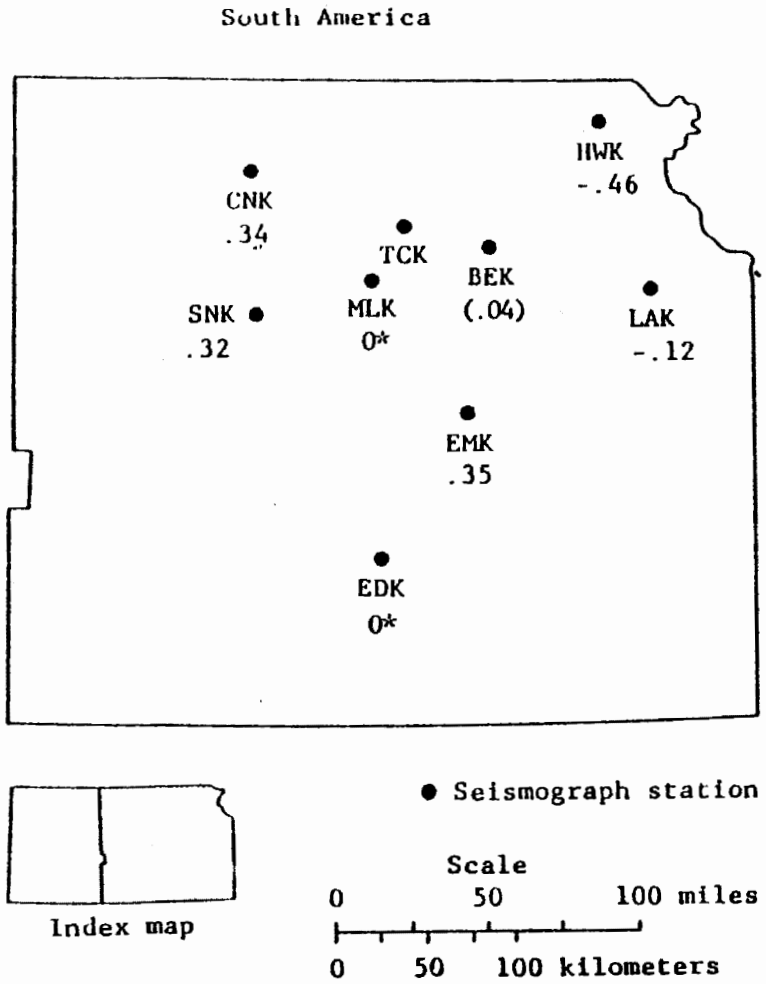

FIG. 6. Average of residuals, relative to TCK, from South American events.

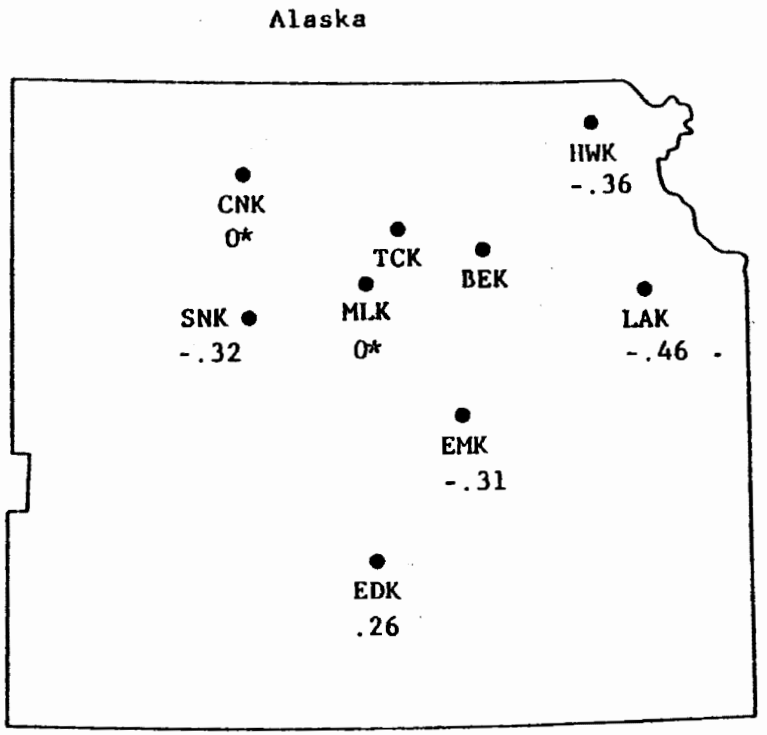

FIG. 7. Average of residuals, relative to TCK, from Alaskan events.

0* implies a zero delay.

( ) indicates that only one event is represented.

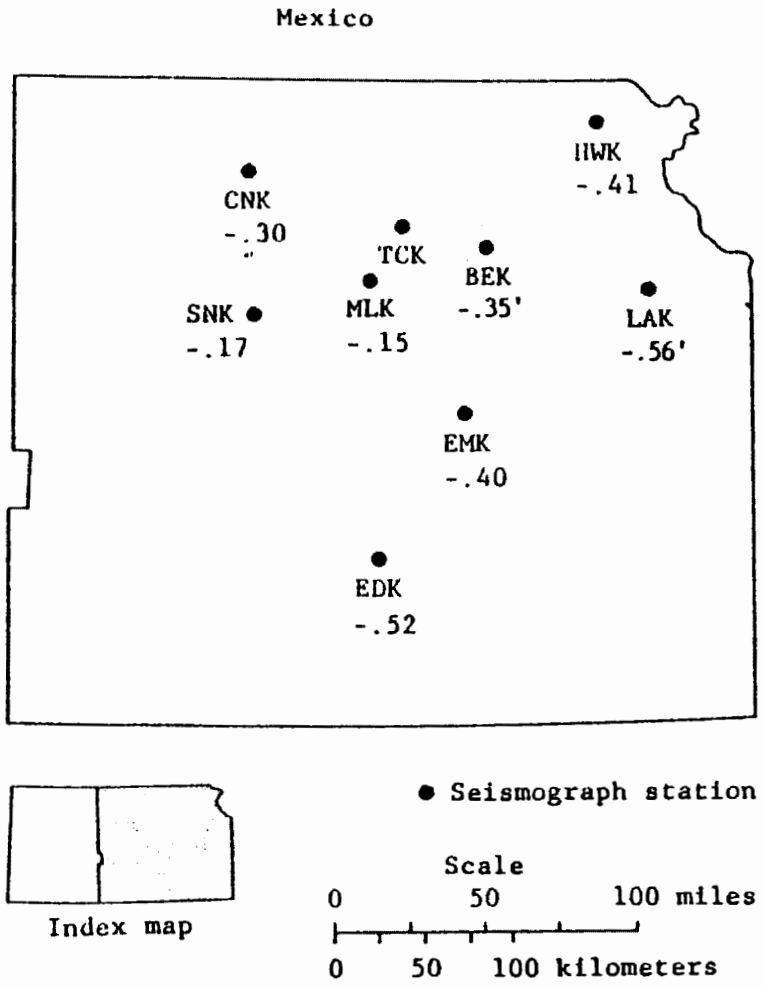

FIG. 8. Average of residuals, relative to TCK, from Mexican events.

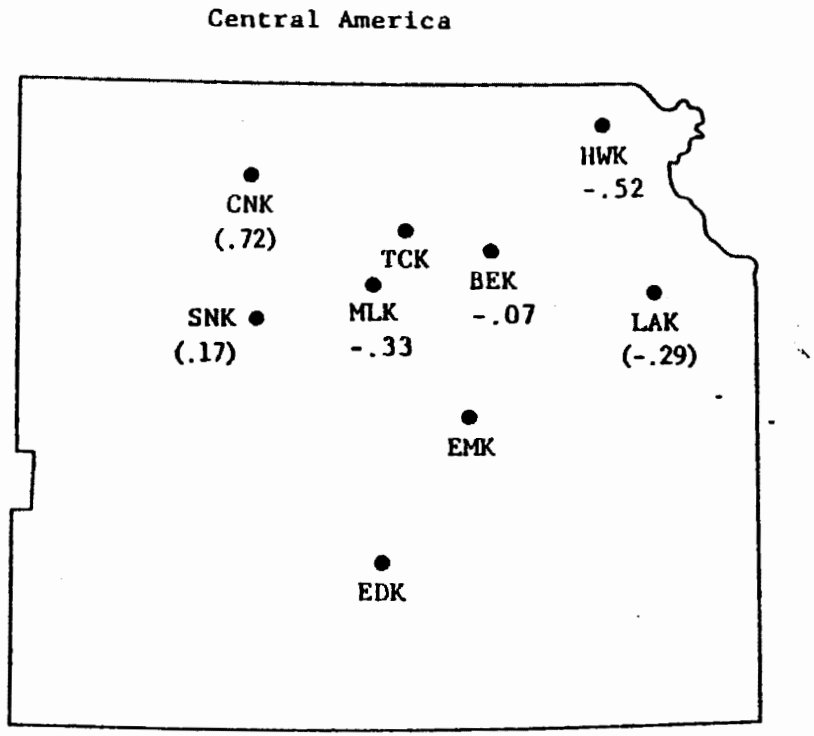

FIG. 9. Average of residuals, relative to TCK, from Central American events.

( ) indicates that only one event is represented.
' indicates a large standard deviation.

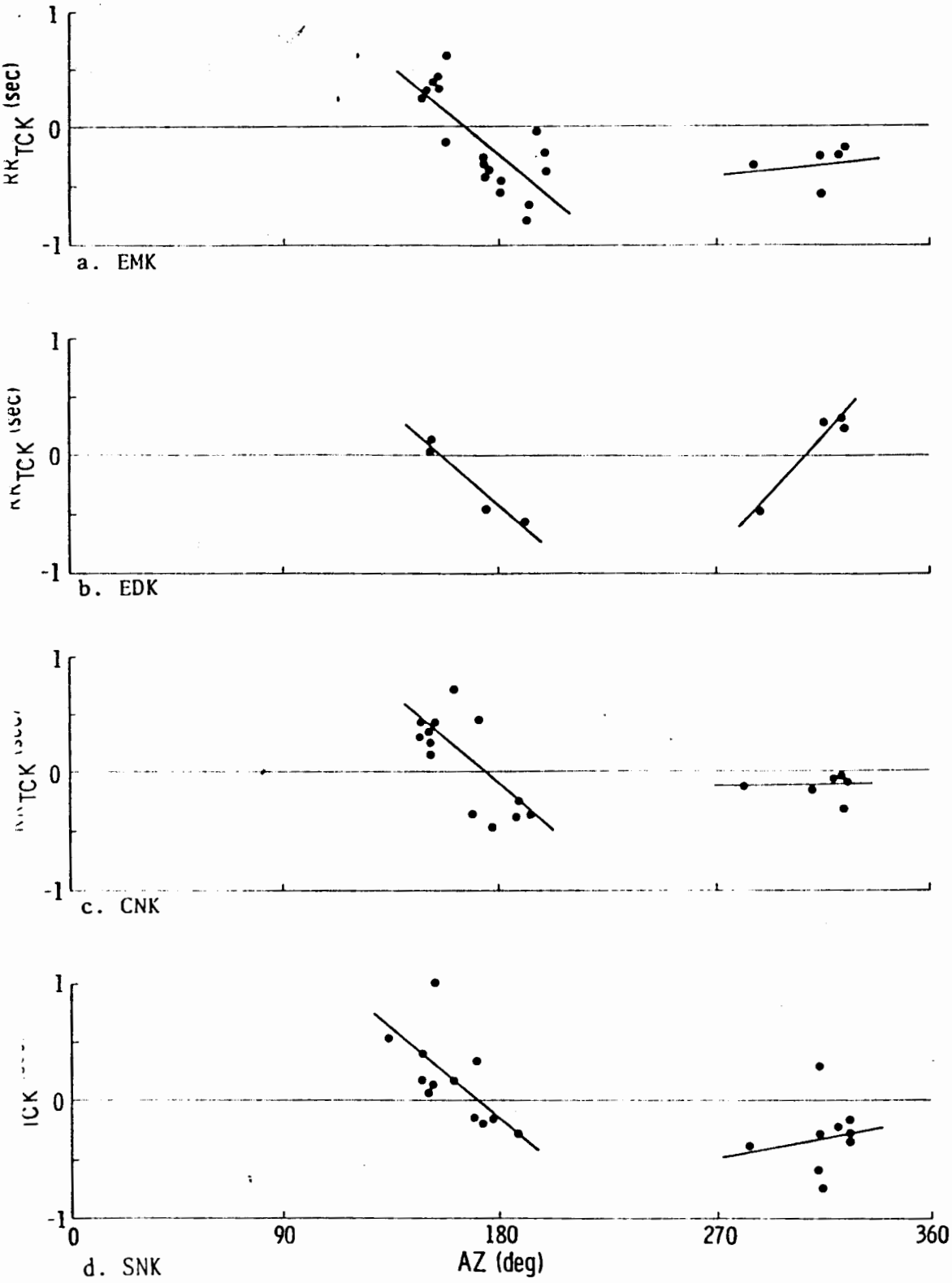

FIG. 10a-10d. Residuals, relative to TCK, plotted against azimuth. Lines are least-squares fits

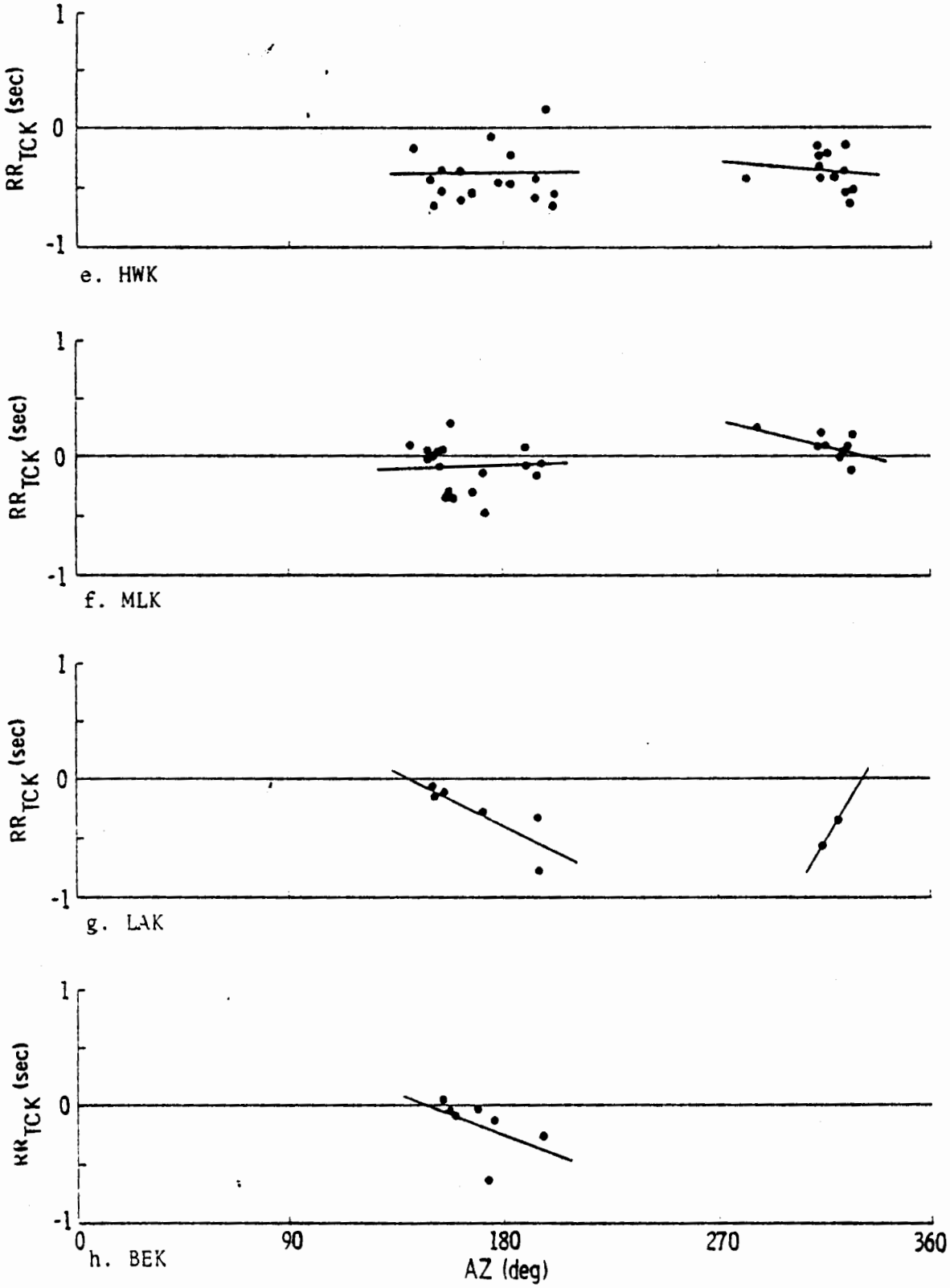

FIG. 10e-10h. Residuals, relative to TCK, plotted against azimuth. Lines are least-squares fits.

TABLE 8. BEST-FIT STRAIGHT LINES* FOR RR_{TCK} vs. AZ GRAPHS

STATION	AZIMUTH LESS THAN 250°			AZIMUTH GREATER THAN 250°		
	m	b	R^2	m	b	R^2
LAK	-.010	1.450	.686	-.017	4.870	.765
BEK	-.008	1.114	.227	-----	-----	----
EMK	-.017	2.883	.577	.002	-.901	.036
HWK	.001	-.552	.004	-.002	.280	.024
MLK	.001	-.238	.015	-.005	1.619	.343
EDK	-.018	2.872	.936	.022	-6.722	.927
SNK	-.017	2.880	.455	.003	-1.299	.020
CNK	-.018	3.066	.530	.001	-.265	.005

* The values b and m are for the equation for a straight line: $y = mx + b$.
R^2 is a statistical measure of fit: $R^2 = 1.0$ implies a perfect fit.

TABLE 9. BEST-FIT SINE CURVES* FOR RR_{TCK} vs. AZ GRAPH

STATION	NUMBER OF OBSERVATIONS	A (sec)	B (sec)	E (deg)
EDK	8	.30	1.27	37.6
CNK	19	.21	.81	21.4
SNK	21	.09	.77	12.8
EMK	23	.12	.98	21.9
HWK	28	-.42	-.07	3.8
MLK	27	-.01	-.12	-87.8
LAK	8	-.20	.63	19.7

* The curves are of the form: $RR = A + B \sin (AZ + E)$.

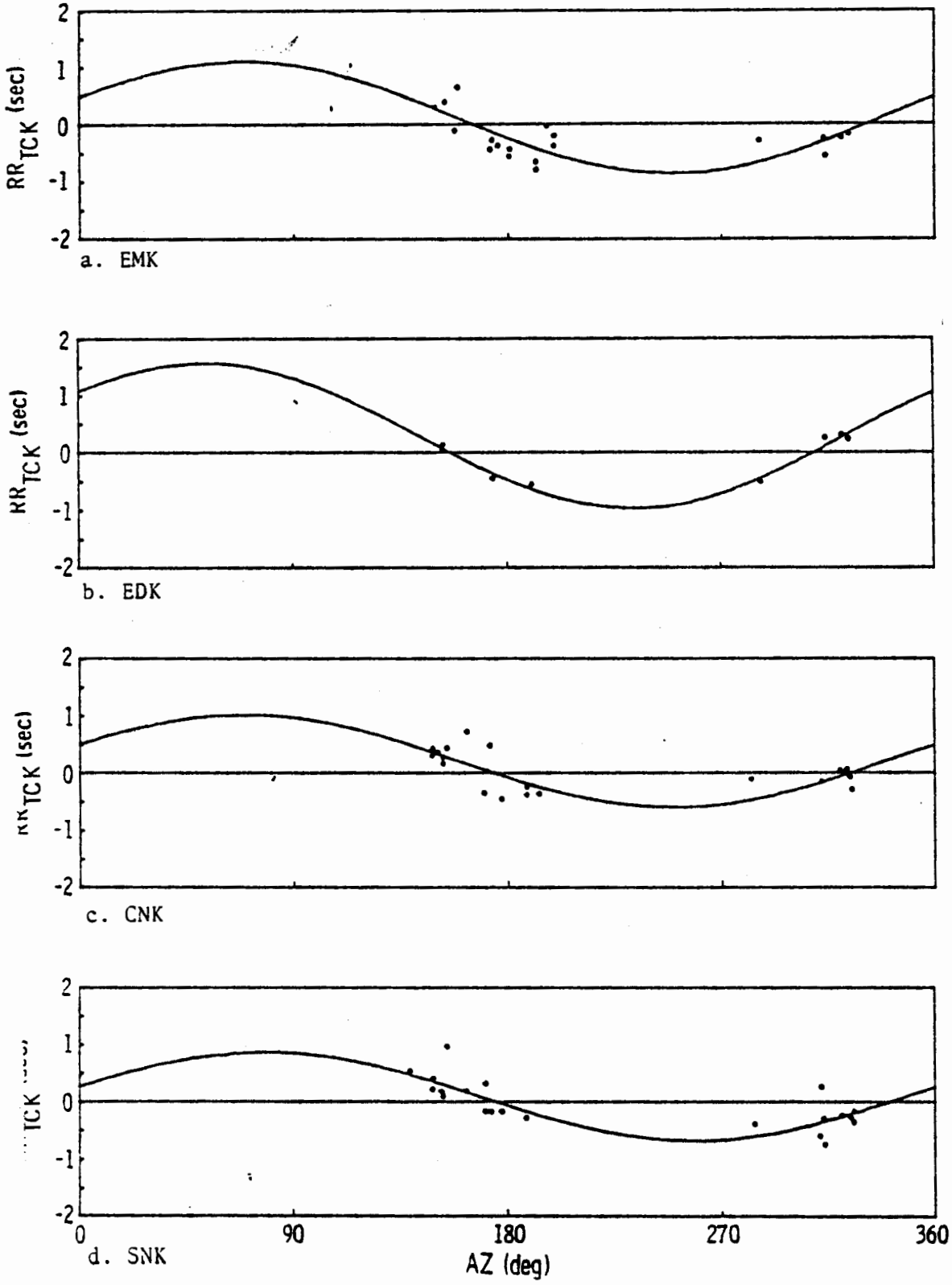

FIG. 11a-11d. Residual anomaly functions for EMK, EDK, CNK, and SNK.

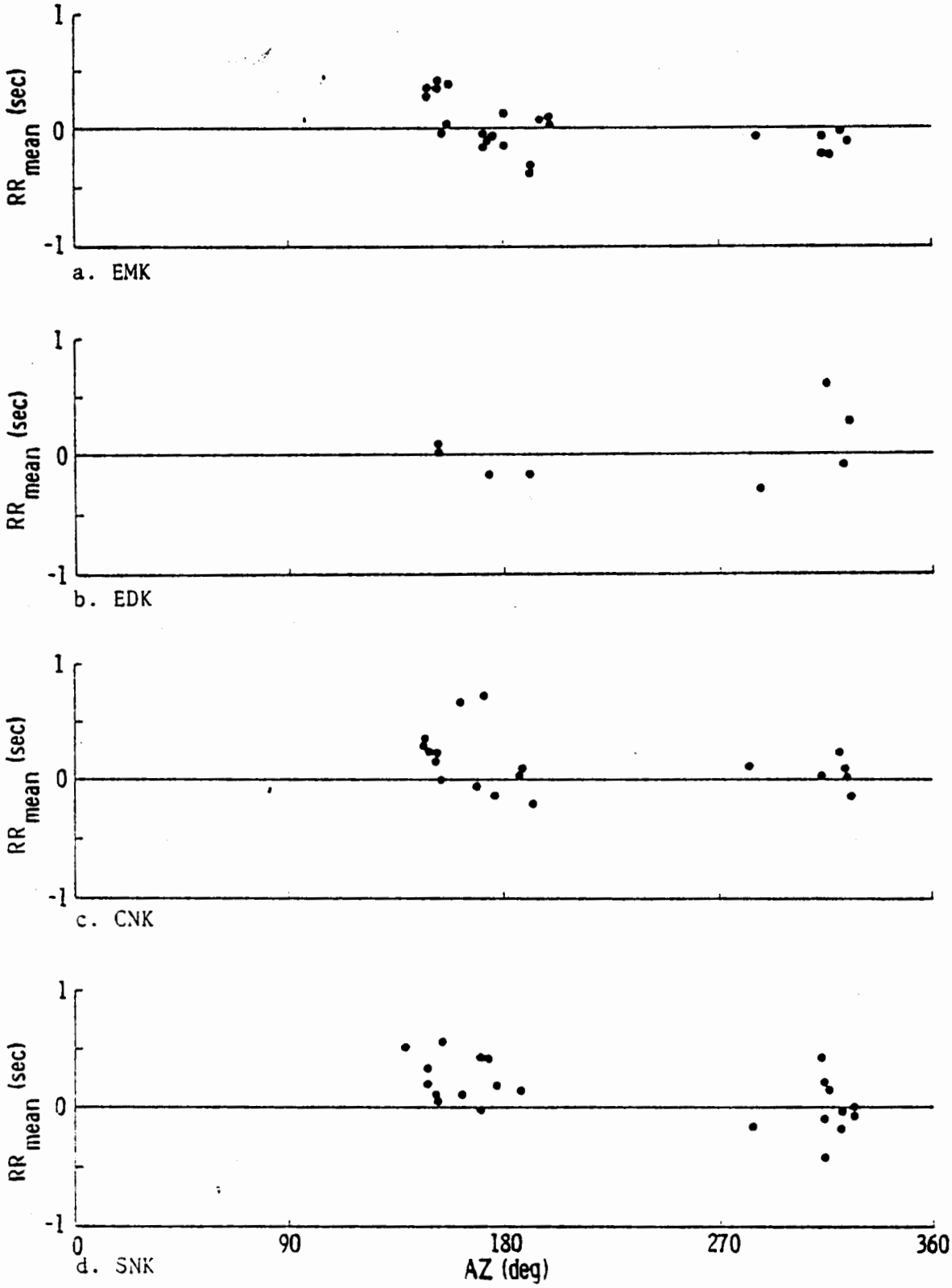

FIG. 12a-12d. Residuals, relative to the mean, plotted against azimuth.

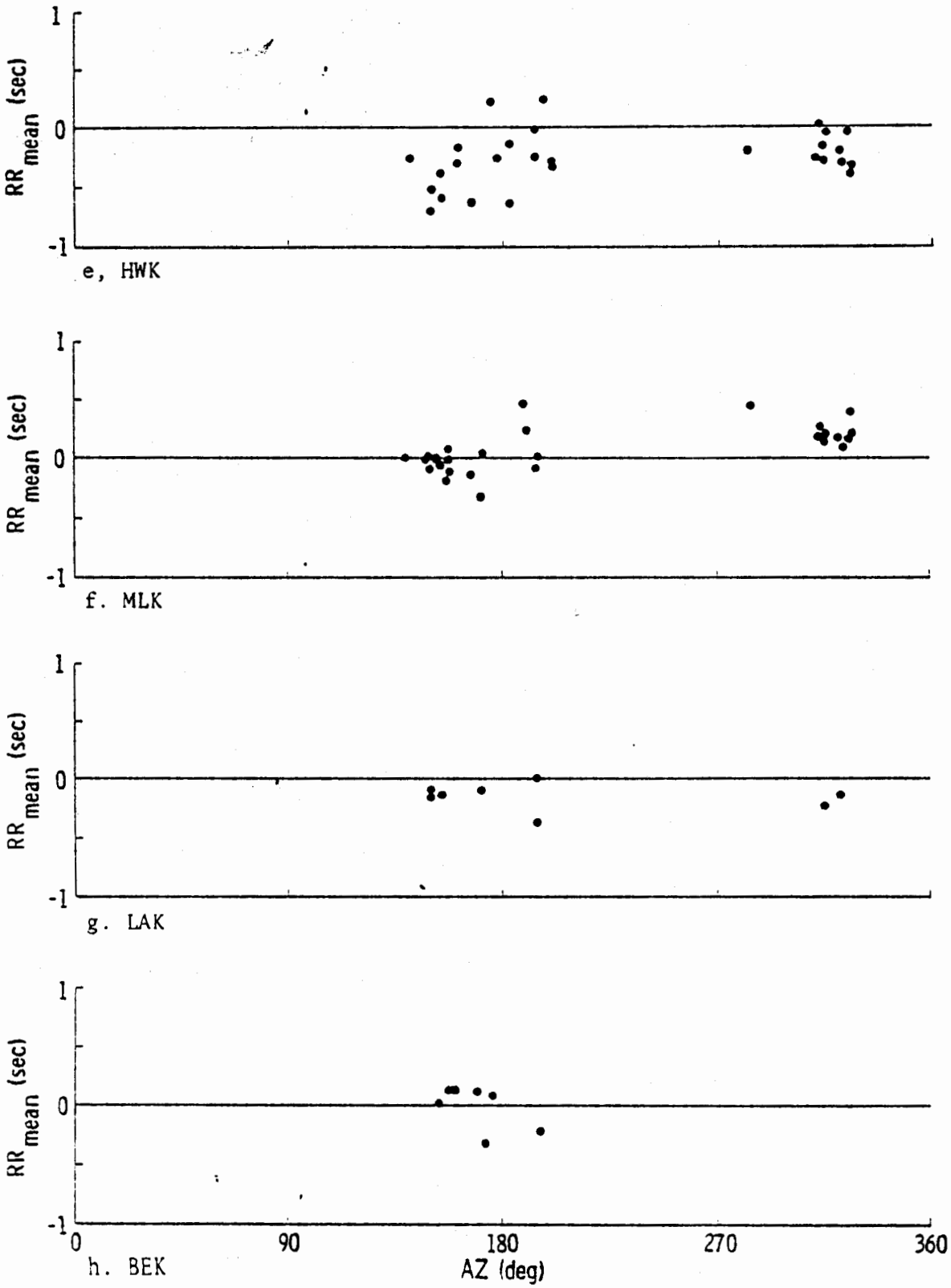

FIG. 12e-12h. Residuals, relative to the mean, plotted against azimuth.

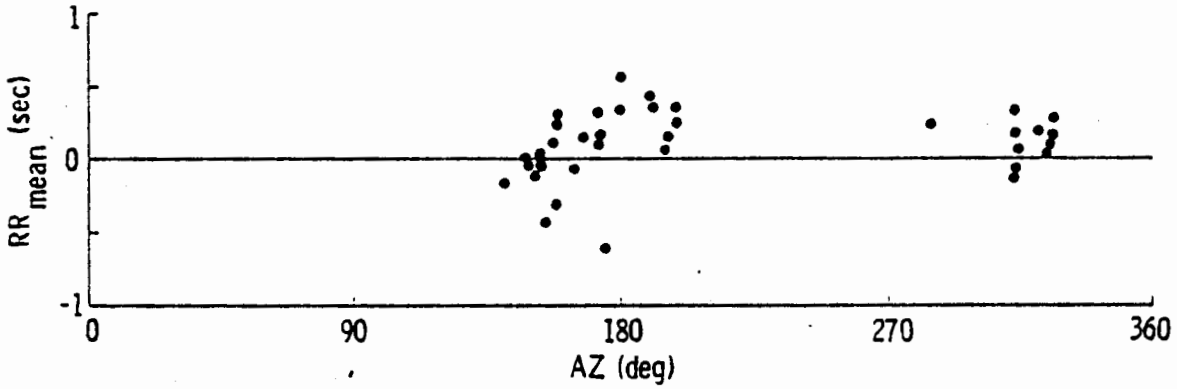

FIG. 12i. Residuals, relative to the mean, plotted against azimuth for TCK.

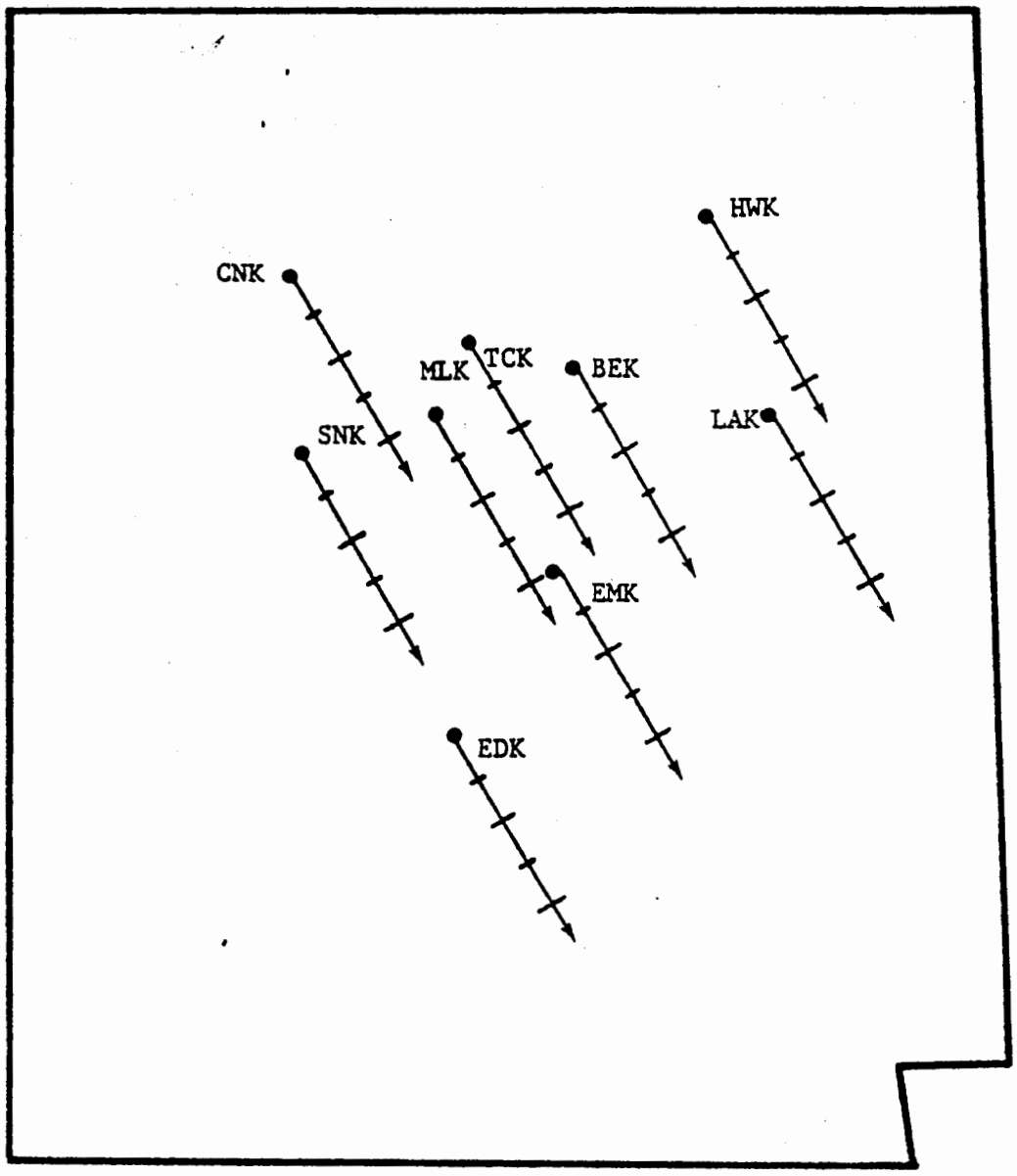

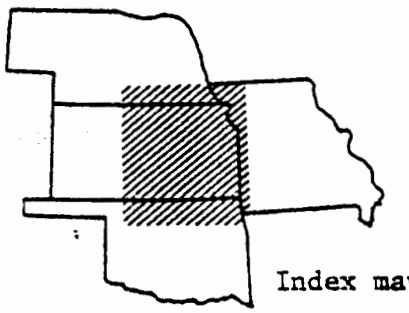

Scale

miles

0 50 100

0 50 100 150

kilometers

FIG. 13. Projections of ray paths (from South American events) on the earth's surface. Each tick mark represents 50 km depth.

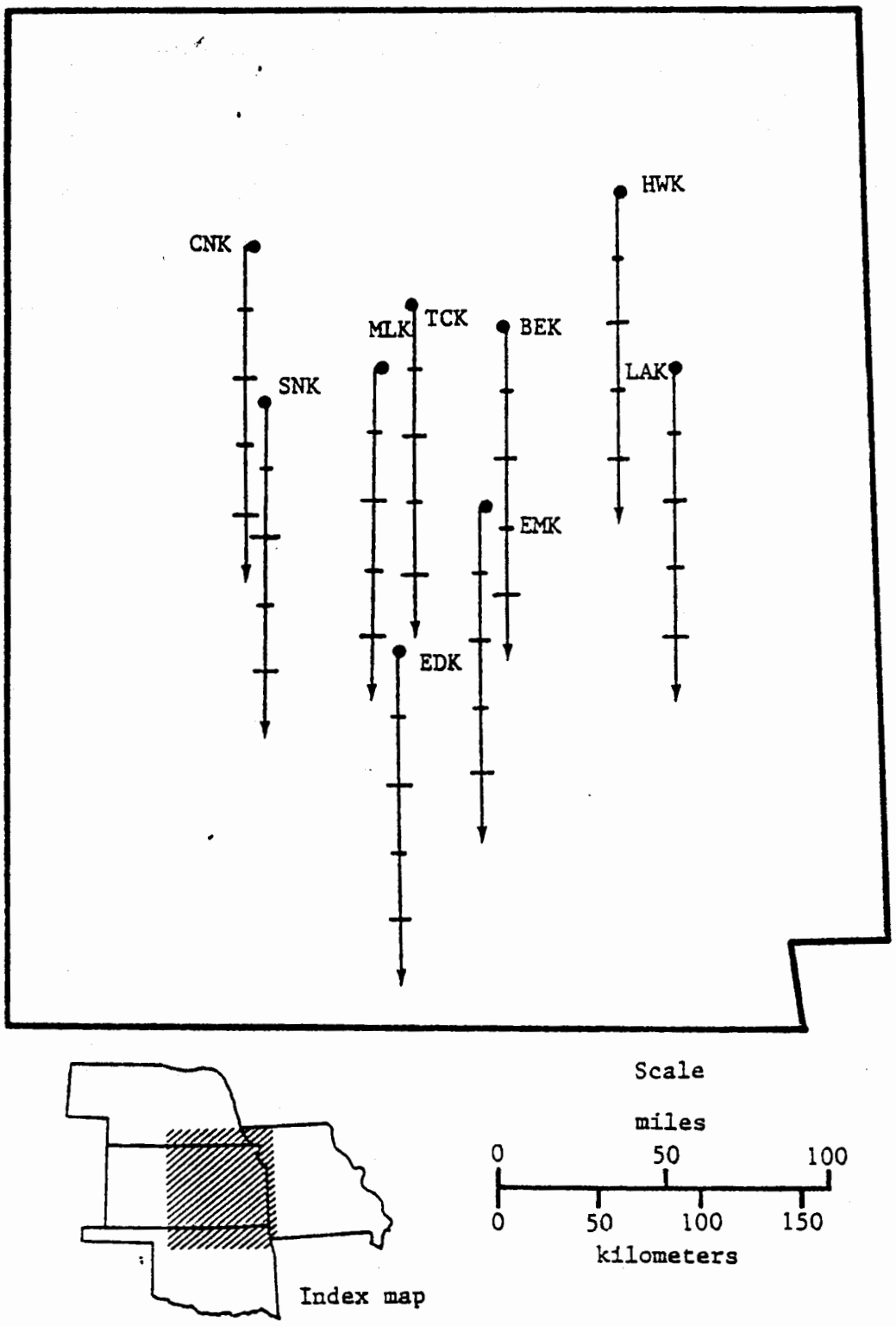

FIG. 14. Projections of ray paths (from Mexican events) on the earth's surface. Each tick mark represents 50 km depth.

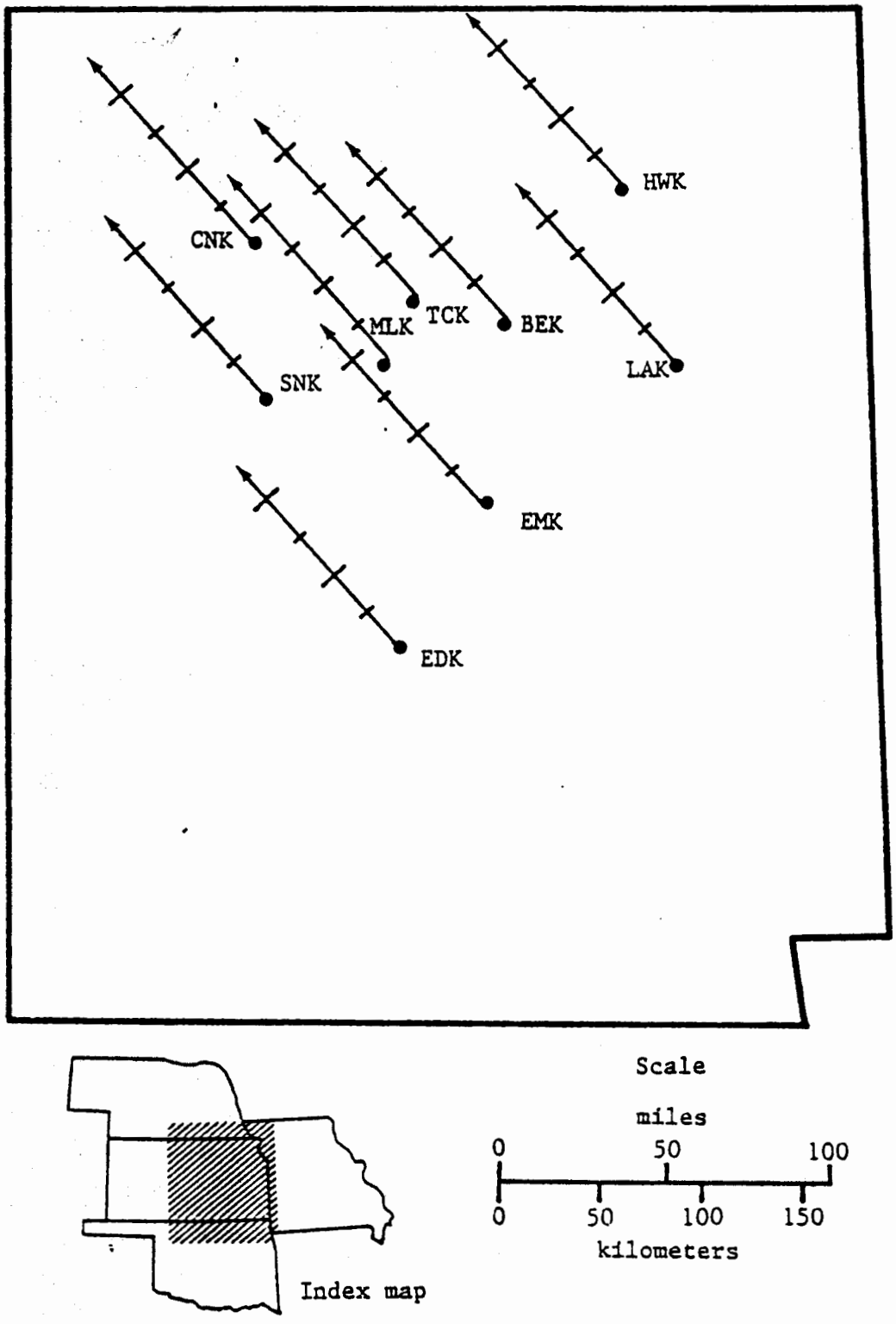

FIG. 15. Projections of ray paths (from Alaskan events) on the earth's surface. Each tick mark represents 50 km depth.

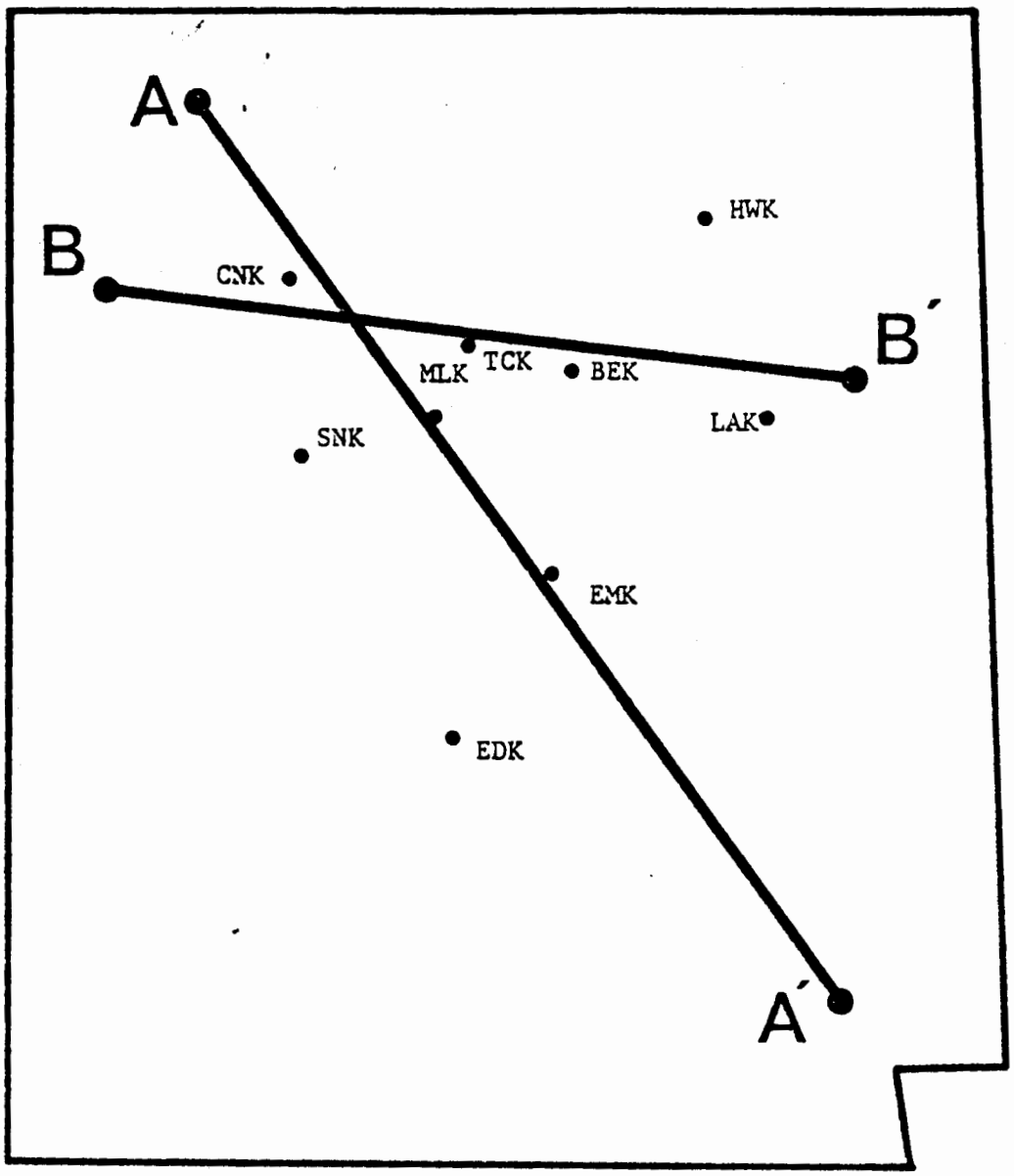

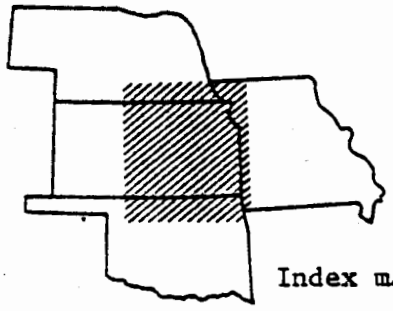

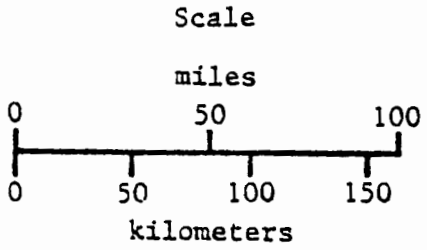

FIG. 16. Location of lines A-A' and B-B' used in Fig. 18 and Fig. 19.

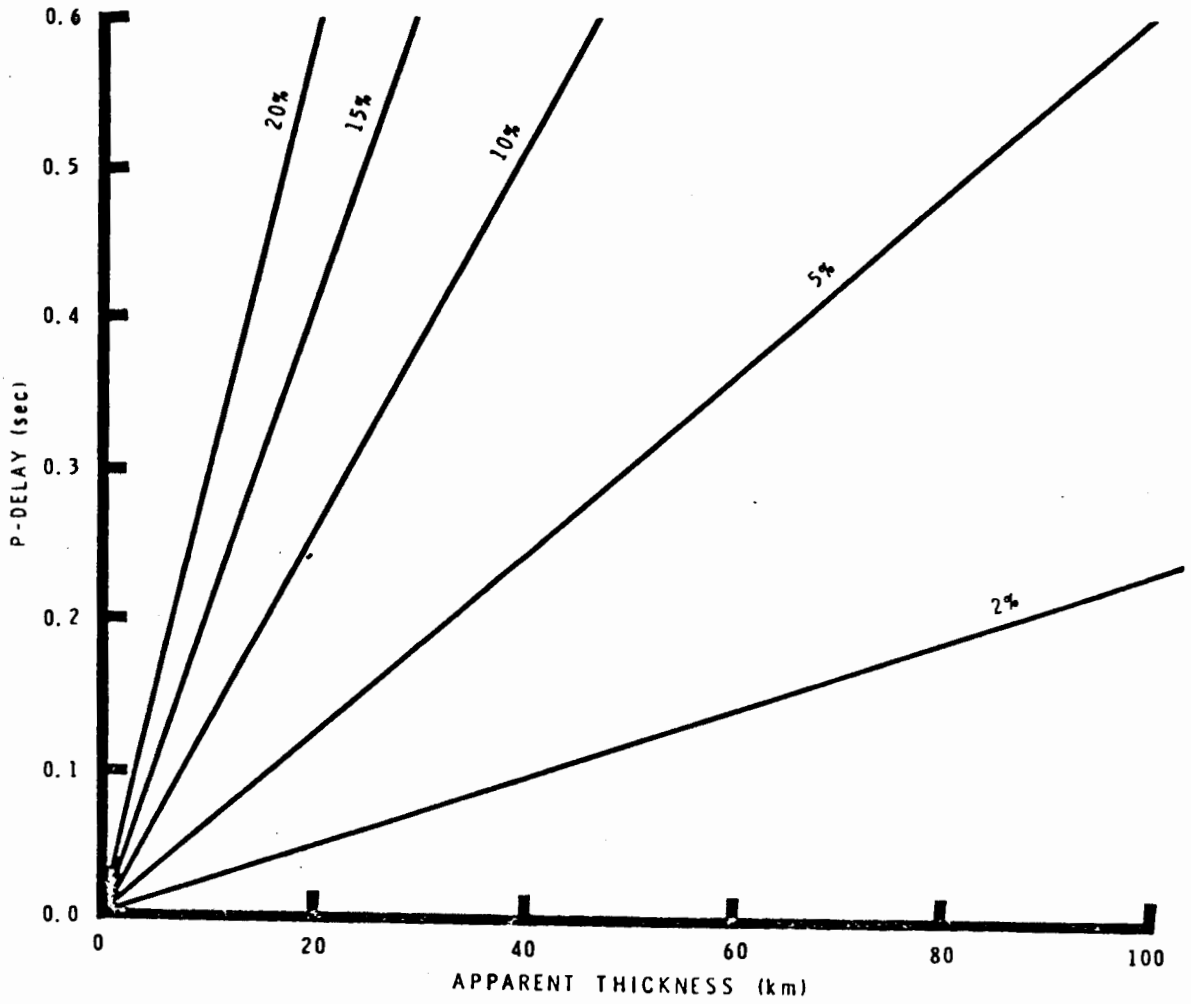
TELESEISMIC P-DELAYS VS. APPARENT THICKNESS
FOR VARIOUS PERCENTAGE VELOCITY DECREASES
ASSUMING NORMAL VELOCITY OF 8.25 km/sec
P-DELAY (sec)
0.6
0.5
0.4
0.3
0.2
0.1
0.0
20%
15%
10%
5%
2%
0
20
40
60
80
100
APPARENT THICKNESS (km)

FIG. 17.

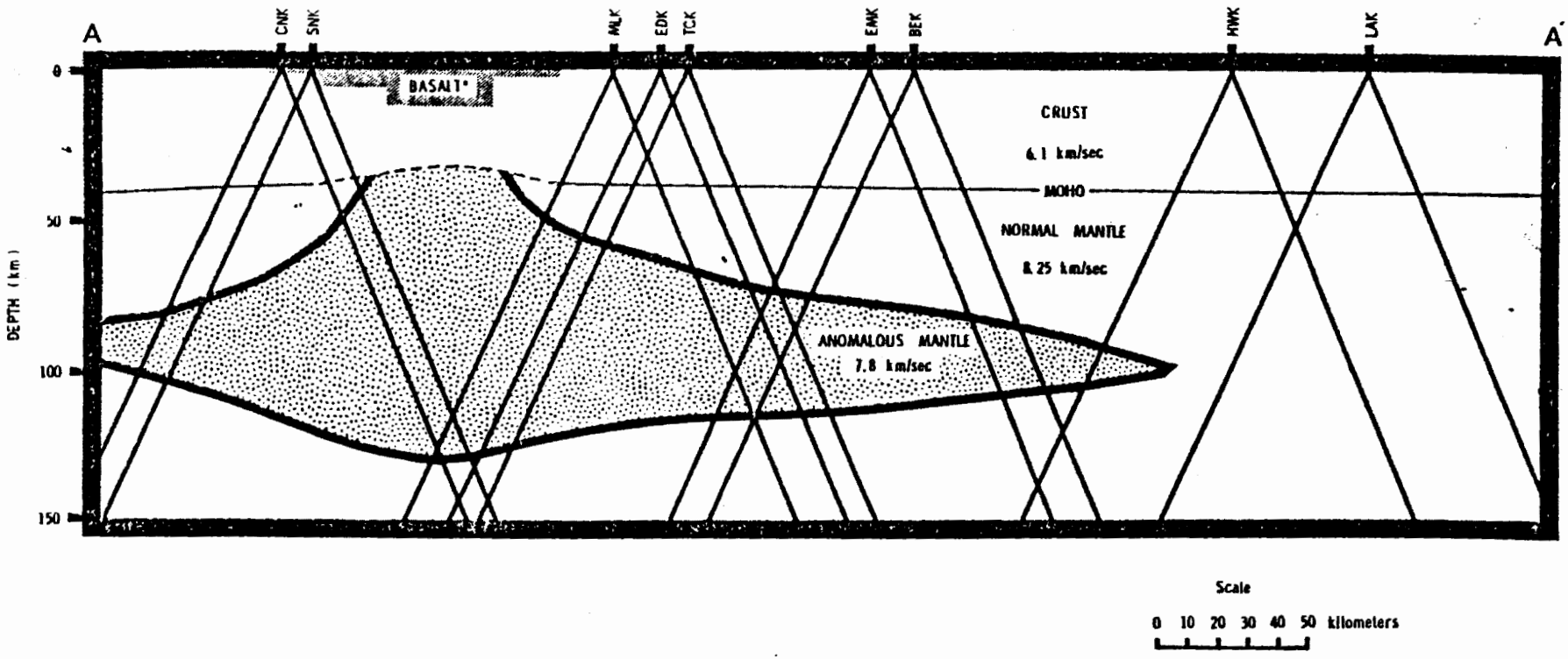

FIG. 18. Crustal and upper mantle cross-section along line A-A' (shown on Fig. 16). Ray paths from Alaskan and South American events are included.

* Basalt is located from Fig. 4.

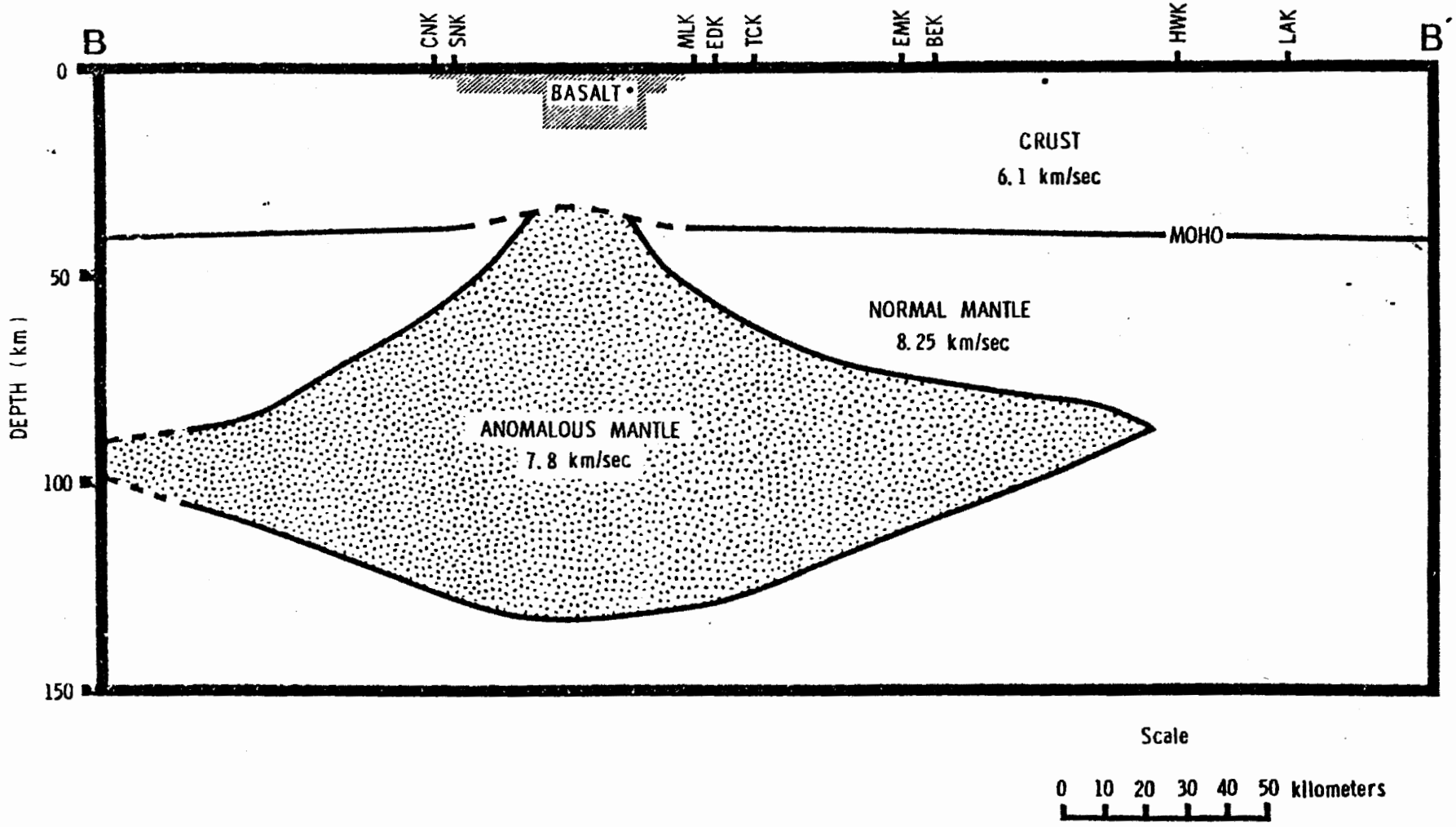

FIG. 19. Crustal and upper mantle cross-section along B-B' (shown on Fig. 16).

* Basalt is located from Fig. 4.

DISCUSSION AND RECOMMENDATIONS

Ibrahim (1963) used seismic refraction and teleseismic data to infer that slightly lower Pn velocities were associated with the MGA, although his conclusion may not be too well-founded. Lui (1980) used travel-time data for microearthquakes in Northwest Kansas and Southwest Nebraska to conclude that there must be a low-velocity zone beneath the MGA (in Kansas) in the uppermost mantle. Lui's work is relevant to this study because be came to a similar conclusion based upon a distinctly different data set.

Suggesting a cause for the low-velocity material may be highly speculative. However, because this anomalous mantle material coincides with the MGA, it may be reasonable to attribute this material to the rifting process. The existence of a low-velocity upper mantle beneath both active and inactive rift systems has been well documented (see Bott, 1965; Talwani et al., 1965; Cann, 1968; Vogt, et. al., 1969; Sipken and Jordan, 1975; Lidiak, 1978). Because of the high heat flow over rift systems, this anomalous material has been almost entirely attributed to partial melt in the crust and upper mantle.

In attempts to explain the rifting process, Wilson (1963) and Morgan (1971) have proposed that hot spots, or melting spots, in the mantle could be used as absolute reference points. The concept of mobil plates combined with relatively stationary hot spots gives an explanation for lithospheric uplift and subsidence. Morgan (1972)

and Deffeyes (1972) have interpreted hot spots in terms of thermal convection; a concentrated upwelling of hot material from the lower mantle, hence the concept of the mantle plume. Such a mantle plume will generate thermal expansions, or bumps, at the base of and within the asthenosphere. These bumps can contribute to uplift, fracture, and magmatism in the overlying lithosphere and, ultimately, to the breakup of continents (Anderson, 1975).

Anderson (1975) has suggested that mantle plumes could be the result of upwelling of primitive material that was intrinsically lighter because of its chemistry. Such chemical plumes would be concentrated in CaO, Al_2O_3, TiO_2, U, and Th relative to the normal mantle. Furthermore, a typical plume assemblage would be rich in CaO, Al_2O_3, TiO_2, CO_2, H_2O and Cl and the refractory trace elements relative to, for instance, the deep oceanic basalts. Rocks characteric of a plume would include anorthosite, kimberlite, carbonatite, and melilite.

It is significant that such an assemblage is thought to be associated with mantle plumes. Not only is the MGA a site of massive mafic intrusive and extrusive rocks, but in addition, kimberlites are present in Kansas and carbonatite is present in Nebraska in the vicinity of the MGA (Figure 20). Because the MGA is thought to represent an ancient rift system and much of Anderson's (1975) plume assemblage is present in the MGA region, there is reason to speculate that the rifting may have been a result of a mantle plume.

Distinguishing between chemical and thermal plumes is generally difficult, as the geophysical and geochemical manifestations of plume activity are about the same for both types of plumes (Anderson, 1975). The major difference between the two plume types, in regards to this study, is the mechanism of heat production. Anderson's (1975) model of chemical plumes explains the thermal anomalies as being the result of high uranium and thorium content in chemical plumes rather than to the tops of upwelling deep mantle thermal convection currents.

This difference in mechanisms of heat production has important implications concerning the origin of the low-velocity material inferred in this study. The radioactivity from the top of a chemical plume would replenish the heat lost from volcansim, creating new molten material. Because the half-lives of uranium and thorium are 4.5 billion years or more, the MGA (1.1 billion years old), assuming a chemical plume origin, should probably be characterized by slightly higher heat flow. However, there is no evidence to support this. In contrast, the heat source of a thermal plume results from convection in the mantle, heated from the lower mantle (Morgan, 1973). In the absence of a heat source, (that is, after the lithosphere has passed over a thermal plume) the remnant heat from the plume would dissipate in about 100 million years (Deffeyes, 1972).

The chemical differences between the thermal plume derived material and normal upper mantle melts must be attributed to different degrees of partial melting and different phase assemblages at depth (Anderson, 1975). The cause of the low-velocity material may

therefore be attributed to residual compositional differences related to the differentiation of magma in the upper mantle. It is impossible to determine whether this magma differentiation is related to plume activity or is restricted to the upper mantle. However, it appears that the thermal plume hypothesis of Morgan (1972) and Deffeys (1972) is preferred over the chemical plume hypothesis of Anderson (1975).

The KGS seismograph network appears to be too small to reveal the total areal extent of the low-velocity body beneath the MGA. In addition, TCK, the reference station, is situated in a less than ideal location because this station is affected by the anomalous body. A serious effort should be made to do a more detailed P-delay study of the MGA. By putting to use the University of Kansas seismograph stations in Western Kansas and Nebraska and some of the St. Louis University stations in Missouri, the maximum east-west extent of the low-velocity body could be established. More important, though, would be the use of the Oklahoma, Nebraska, and Iowa networks to see whether or not a mantle low-velocity zone exists in conjunction with the MGA in those states. A good reference station, located well away from the MGA, could be used to bypass the interpretation problem associated with TCK.

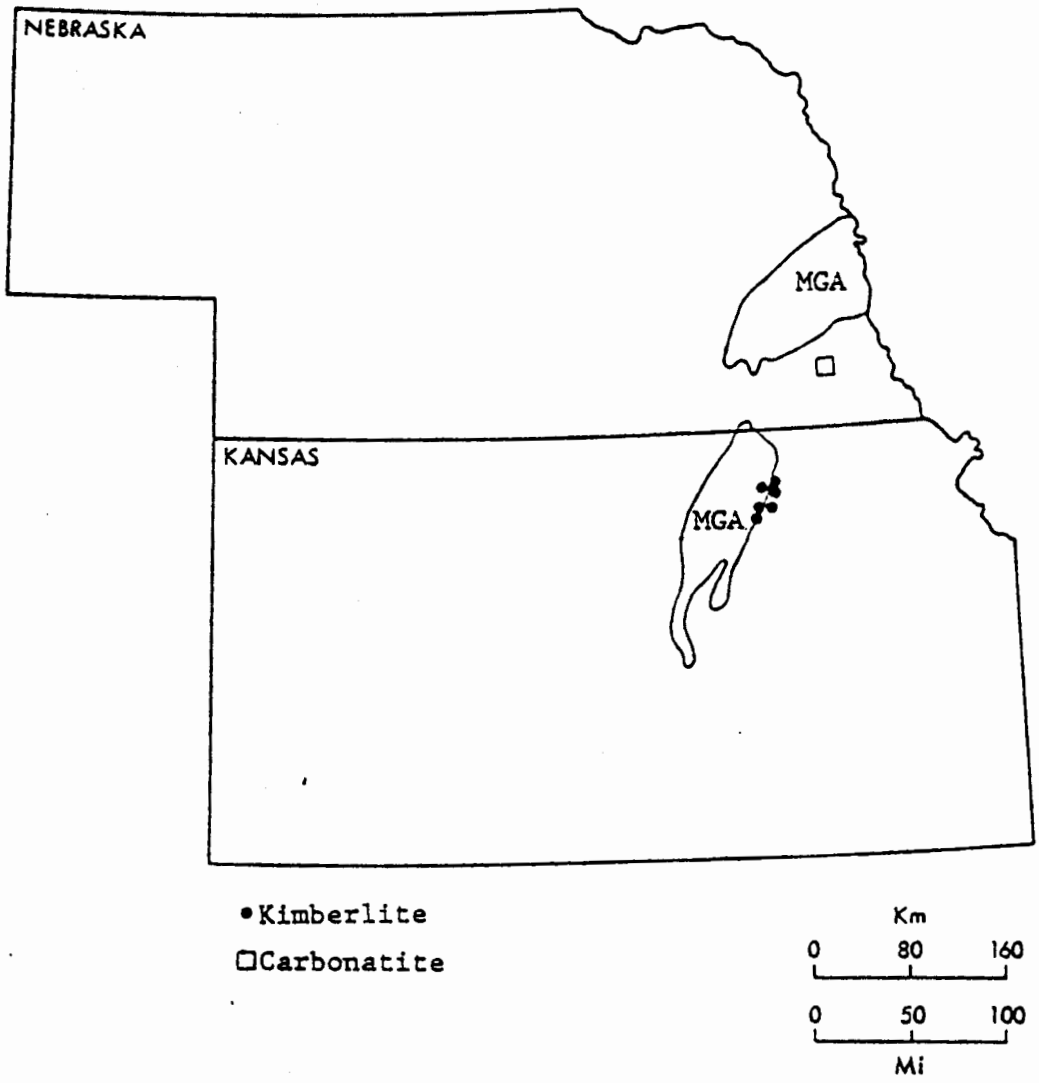

FIG. 20. Locations of kimberlites in Kansas and carbonatite in Nebraska.

APPENDIX A

HYPOCENTER , ORIGIN TIME , AND P-WAVE ARRIVAL TIMES

NO	REFERENCE STATIONS								
	* LOCALITY	DATE	ORIGIN TIME		LATITUDE		LONGITUDE		DEPTH
		ARRIVAL TIMES							
	STATION	HR.	MIN.	SEC.	COMMENTS				
1	MULT MLK TCK BEK LAK								
	*GUATEMALA	FEB2278	6.	7. 37.0	14.	14.9	91.	22.7	100.
	MLK	6.	12.	55.55	BF				
	TCK	6.	12.	58.05	AF				
	BEK	6.	12.	56.20	BF				
	LAK	6.	12.	52.80	BF				
	NEWEVENT								
2	MULT HWK CNK MLK TCK EDK								
	*C ALASKA	MAY0578	5.	32. 47.4	63.	18.1	150.	58.3	134.
	SNK	5.	40.	8.80	CZ				
	MLK	5.	40.	10.70	AZ				
	HWK	5.	40.	10.40	AZ				
	TCK	5.	40.	9.20	BZ				
	CNK	5.	40.	4.50	AZ				
	NEWEVENT								
3	MULT TCK HWK MLK BEK								
	*NICARAGUA	JUL2078	9.	34. 47.2	12.	9.0	86.	37.7	121.
	TCK	9.	40.	33.40	A?				
	HWK	9.	40.	33.70	A?				
	MLK	9.	40.	31.20	A?				
	BEK	9.	40.	31.05	C TIME?				
	NEWEVENT								
4	MULT TCK MLK EMK SNK CNK								
	*COASTCHILE	AUG0378	18.	11. 17.1	-26.	30.8	70.	32.6	58.
	TCK	18.	22.	23.00	CF?				
	EMK	18.	22.	17.30	BF				
	SNK	18.	22.	23.45	BF				
	CNK	18.	22.	26.20	BF				
	NEWEVENT								
5	MULT TCK EMK MLK BEK SNK								
	*COSTARICA	AUG2378	0.	38. 32.2	10.	12.2	85.	13.3	56.
	TCK	0.	44.	44.50	BZ				
	EMK	0.	44.	35.70	BZ				
	MLK	0.	44.	42.40	BZ				
	BEK	0.	44.	42.21	CZ				
	NEWEVENT								

```
 6 MULT MLK  SNK  TCK  EMK
  *MEXICO  SEP0278  16.  3. 44.2 16.  56.8     93.  44.3     125.
   MLK   16.   8.    33.20     BZ
   SNK   16.   8.    33.35     BZ
   TCK   16.   8.    36.15     BZ
   EMK   16.   8.    26.30     AZ

  NEWEVENT
 7 MULT TCK  SNK  MLK  HWK  EMK
  *MEXICO  SEP2978   16. 21. 41.  18.  36.9    102.  15.7      96.
   TCK   16.  26.    21.15     CZ
   EMK   16.  26.    12.60     AZ
   MLK   16.  26.    17.90     CZ
   HWK   16.  26.    28.10     AZ
   BEK   16.  26.    20.80     CZ

  NEWEVENT
 8 MULT TCK  EMK  HWK
  *COAST MEX OCT2278 14.  7.  0.2 15.  10.6    104.  26.9      33.
   HWK   14.  12.    31.45     BZ
   EMK   14.  12.    17.90     BZ
   TCK   14.  12.    25.60     BZ LP

  NEWEVENT
 9 MULT TCK  EMK  HWK
  *COAST MEX OCT2278A14. 17. 14.4 15.  18.8    104.  29.2      33.
   HWK   14.  22.    44.60     BZ
   EMK   14.  22.    31.05     CZ
   TCK   14.  22.    38.60     BZ

  NEWEVENT
10 MULT TCK  SNK  MLK  HWK  EMK
  *ARGENTINA OCT2778 10.  6. 46.1-21.  54.4     65.  47.5     280.
   TCK   10.  17.    13.25     AF
   SNK   10.  17.    13.45     AF
   CNK   10.  17.    16.80     BF
   MLK   10.  17.    12.20     AF
   HWK   10.  17.    12.00     AF
   EMK   10.  17.    07.45     AF
   LAK   10.  17.     7.55     CF .25SECLATER

  NEWEVENT
11 MULT EMK  CNK  HWK  TCK  SNK
  *SO MEXICO NOV2978A19. 52. 47.6 16.   0.6     96.  35.5      18.
   TCK   19.  57.    56.30     AF LP
   EMK   19.  57.    46.45     AF
   SNK   19.  57.    52.10     CF
   EDK   19.  57.    40.60     CF?
   HWK   19.  58.    00.10     BF
   CNK   19.  57.    57.30     BF

  NEWEVENT
```

```
12 MULT EMK  MLK  HWK  TCK
  *SO MEXICO NOV2978B20. 49. 48.8 16.  11.1     96.  37.8      22.
   TCK   20.  54.    55.50     AZ
   EMK   20.  54.    45.70     BZ
   HWK   20.  54.    58.65     BZ

  NEWEVENT
13 MULT EMK  MLK  HWK  TCK  SNK
  *SO BOLIVA DEC0578 18. 32. 43.6-20.  45.5     66.  29.8      198.
   MLK   18.  43.    10.60     CZ
   HWK   18.  43.    10.25     AZ
   LAK   18.  43.     5.85     CZ
   EMK   18.  43.     5.80     AZ
   CNK   18.  43.    15.30     BZ 15.50
   TCK   18.  43.    11.65     BZ
   SNK   18.  43.    12.00     BZ

  NEWEVENT
14 MULT EMK  CNK  HWK  TCK  SNK
  *EL SALVADORDEC067811. 53. 34.0 13.   8.7     89.  38.1      33.
   TCK   11.  59.    15.20     BZ
   CNK   11.  59.    19.00     BZ
   HWK   11.  59.    16.25     AZ
   SNK   11.  59.    13.45     CZ

  NEWEVENT
15 MULT MLK  TCK  BEK
  *PERU    JAN0679    1. 31. 47.6- 8.  53.0     75.  43.7      33.
   MLK    1.  40.    53.65     BF
   TCK    1.  40.    55.00     CF
   BEK    1.  40.    52.90     CF

  NEWEVENT
16 MULT MLK  TCK       CNK
  *MICH MEX JAN0679A 11. 51. 30.7 18.  16.2    102.  47.1      32.
   TCK   11.  56.    22.20     CF
   MLK   11.  56.    19.00     BF
   CNK   11.  56.    21.15     BF

  NEWEVENT
17 MULT EMK  MLK  TCK  HWK  CNK
  *MEXICO   JAN1079  13. 24. 14.3 16.  56.6     93.  32.6      156.
   TCK   13.  29.     2.70     CF
   CNK   13.  29.     4.75     CF 5.2A
   EMK   13.  28.    52.80     CF
   HWK   13.  29.     5.60     AF
   BEK   13.  29.     0.40     BF

  NEWEVENT
```

```
18 MULT MLK  SNK  TCK  HWK
  *NCOLOMBIA JAN1479 19. 20. 30.2  6.  44.8     72.  59.1     164.
   MLK   19.  28.     5.87     AFD EYE
   SNK   19.  28.     8.43     AFU
   TCK   19.  28.     6.76     AFD
   HWK   19.  28.     4.51     AFU

  NEWEVENT
19 MULT EMK  MLK  TCK  HWK
  *ALU ISLS JAN2579A 17.  5. 44.7 52.  30.9    176.   2.5     156.
   TCK   17.  14.     52.90     AF
   MLK   17.  14.     53.80     AF
   HWK   17.  14.     55.75     AF
   SNK   17.  14.     51.65     BF

  NEWEVENT
20 MULT MLK  CNK  EMK  TCK  HWK
  *SO ALASKA JAN2579 19. 30. 06.1 60. 07.9     153.  07.3     105.
   LAK   19.  37.     49.52     BIZ
   MLK   19.  37.     42.57     AIZ
   CNK   19.  37.     36.78     BIZ
   EDK   19.  37.     51.18     CEZ
   EMK   19.  37.     48.88     BIZ
   SNK   19.  37.     40.46     BIZ
   TCK   19.  37.     41.52     AIZ
   HWK   19.  37.     43.56     CIZ

  NEWEVENT
21 MULT MLK  CNK  EMK  TCK  HWK
  *MEXICO JAN2679    10. 04. 32.0 17. 24.8     100.  52.6      29.
   LAK   10.   9.     31.92     DEAD
   MLK   10.   9.     29.87     AIZ
   CNK   10.   9.     32.82     AEZ
   EMK   10.   9.     23.47     BE MISS P
   TCK   10.   9.     33.01     AEZ
   HWK   10.   9.     38.54     BEZ

  NEWEVENT
22 MULT MLK  CNK  EMK  TCK  HWK
  *ALASKA PN JAN2779 18. 57. 55.0 54.  46.1    161.  15.0      50.
   MLK   19.   6.     25.73     AIZ
   CNK   19.   6.     19.65     AEZ
   EMK   19.   6.     31.53     DEZ
   SNK   19.   6.     22.98     AIZ
   TCK   19.   6.     24.93     AIZ
   HWK   19.   6.     27.91     CIZ2

  NEWEVENT
```

```
23 MULT TCK  CNK  EMK  MLK  HWK
  *COAST CAL FEB0379  9. 58. 16.1 40.  53.4    124.  24.8      28.
   MLK   10.   2.    58.01     AIZ
   CNK   10.   2.    50.04     BEZ
   EDK   10.   2.    61.82     CEZ
   EMK   10.   2.    63.80     AIZ
   SNK   10.   2.    52.06     AEZ
   TCK   10.   2.    58.46     AIZ
   HWK   10.   2.    66.78     CIZ?

  NEWEVENT
24 MULT MLK  CNK  EMK  TCK  HWK
  *ALASKA PN FEB1379  5. 34. 25.9 55.  27.2    157.   9.7      33.
   LAK    5.  42.    36.43     C
   EDK    5.  42.    37.10     C
   EMK    5.  42.    34.67     C
   SNK    5.  42.    25.80     C
   TCK    5.  42.    28.17     C
   HWK    5.  42.    31.21     C

  NEWEVENT
25 MULT MLK  CNK  EMK  TCK  HWK
  *PERUCOAST FEB1679 10.  8. 53.4-16.  23.4     72.  39.5      53.
   LAK   10.  18.    50.30     DEZ
   MLK   10.  18.    54.81     AIZ
   CNK   10.  18.    59.48     AIZ
   EDK   10.  18.    46.49     AIZ
   EMK   10.  18.    49.76     AIZ
   SNK   10.  18.    55.77     AIZ
   TCK   10.  18.    56.09     AIZ
   HWK   10.  18.    55.45     AIZ?

  NEWEVENT
26 MULT MLK  CNK  SNK  TCK  HWK
  *PERUCOAST FEB1779 22. 18. 20.0-16.  30.0     72.  39.4      52.
   EDK   22.  28.    14.42     CEZ
   MLK   22.  28.    22.64     AIZ
   CNK   22.  28.    27.41     CEZ
   EMK   22.  28.    17.59     AIZ
   SNK   22.  28.    23.64     DEZ
   TCK   22.  28.    23.92     AIZ
   HWK   22.  28.    23.09     BIZ

  NEWEVENT
27 MULT MLK  CNK  SNK  TCK  HWK
  *ALASKA FEB1779A   10. 48.  8.7 62.  18.4    149.  29.8      54.
   MLK   10.  55.    32.89     AIZ
   CNK   10.  55.    26.94     AIZ
   SNK   10.  55.    30.91     AIZ
   TCK   10.  55.    31.58     AIZ
   HWK   10.  55.    33.37     AIZ

  NEWEVENT
```

```
28 MULT MLK  CNK  SNK  TCK  HWK
  *MICH MEX  FEB2279  9. 16. 37.  19.  58.8    100.  16.1      51.
   LAK    9.  21.    18.43     CEZ
   MLK    9.  21.    16.83     AIZ
   CNK    9.  21.    19.90     AIZ
   EDK    9.  21.    01.09     CEZ?
   EMK    9.  21.     9.47     CEZ
   SNK    9.  21.    13.86     DEZ
   TCK    9.  21.    20.13     AIZ
   HWK    9.  21.    26.37     CIZ?

  NEWEVENT
29 MULT TCK  MLK  EMK  HWK  EDK
  *SO ALASKA FEB2879 21. 27. 08.6 60.  39.0    141.  36.6      27.
   MLK   21.  33.    59.70     A
   CNK   21.  33.    53.66     C
   EDK   21.  34.    09.49     A
   EMK   21.  34.    06.33     A
   TCK   21.  33.    58.42     A
   HWK   21.  34.    00.24     C

  NEWEVENT
30 MULT EMK  MLK  TCK  HWK  CNK
  *NICARAGUA MAY1379 22. 43. 16.3 12.   4.1     86.  22.       209.
   EMK   22.  48.    47.70     AZ
   TCK   22.  48.    55.80     AZ
   MLK   22.  48.    54.25     AZ

  NEWEVENT
31 MULT EMK  MLK  TCK  HWK  CNK
  *MEX COAST JUN0479  6. 26. 42.7 15.  41.      93.  35.8       80.
   MLK    6.  31.    48.35     AZ
   TCK    6.  31.    50.90     AZ
   SNK    6.  31.    47.70     AZ
   EMK    6.  31.    41.30     BZ

  NEWEVENT
32 MULT EMK  MLK  TCK  HWK  CNK
  *MEXICO  JUN2279    6. 30. 54.3 17.   0.      94.  36.5      107.
   HWK    6.  35.    47.65     AF
   CNK    6.  35.    47.25     AF
   SNK    6.  35.    41.40     AF
   EDK    6.  35.    28.10     AF
   EMK    6.  35.    34.70     AF
   TCK    6.  35.    43.80     AF
   BEK    6.  35.    43.00     BF TIME?

  NEWEVENT
```

```
33 MULT HWK  MLK  TCK  CNK  SNK
  *C ALASKA JUL1079  4.  4. 20.5 63.  12.1    150.  43.4      130.
   HWK    4.  11.    42.75     BZ 42.90
   SNK    4.  11.    41.05     BZ
   MLK    4.  11.    42.85     BZ?
   TCK    4.  11.    41.65     BZ??

  NEWEVENT
34 MULT HWK  MLK  TCK
  *NICARAGUA DEC1879 10. 37. 54.4 11.  23.5     86.  29.5      33.
   MLK   10.  43.    53.80     B
   HWK   10.  43.    56.00     B
   TCK   10.  43.    55.90     B

  NEWEVENT
35 MULT HWK  MLK  TCK  CNK  SNK
  *ALEU IS FEB1880   11. 15.  1.7 51.  13.9    178.  19.4      50.
   SNK   11.  24.    34.30     BZ
   TCK   11.  24.    35.35     BZ
   HWK   11.  24.    38.35     BZ

  NEWEVENT
36 MULT TCK  HWK  MLK  BEK  CNK
  *PERU-BRAZ APR0480  6. 25. 25. -07.  53.4     74.  24.3      151.
   TCK    6.  34.    15.80     AIF
   MLK    6.  34.    14.50     AAIF
   BEK    6.  34.    14.75     BIF?
   CNK    6.  34.    19.80     AIF

  NEWEVENT
37 MULT TCK  HWK  MLK
  *ALEUTIAN  MAY0380  9. 30. 10.3 51.  12.0   -173.  48.0      51.
   TCK    9.  40.    16.20     AIZ
   HWK    9.  40.    18.70     AIZ
   MLK    9.  40.    16.95     AIZ

  NEWEVENT
```

APPENDIX B

RESIDUALS FOR EDK RELATIVE TO TCK AND THE MEAN

EVENT NUMBER	LOCALITY	AZIMUTH (deg)	RESIDUAL RELATIVE TO TCK (sec)	RESIDUAL RELATIVE TO MEAN (sec)
25	Peru	152.6	.03	.01
26	Peru	152.6	.13	.08
28	Mexico	190.6	-.60	-.17
33	Mexico	174.1	-.45	-.19
20	Alaska	321.1	.28	-.10
24	Alaska	314.1	.26	.59
29	Alaska	323.9	.22	.26
23	California	286.9	-.51	-.29

RESIDUALS FOR LAK RELATIVE TO TCK AND THE MEAN

EVENT NUMBER	LOCALITY	AZIMUTH (deg)	RESIDUAL RELATIVE TO TCK (sec)	RESIDUAL RELATIVE TO MEAN (sec)
10	Argentina	150.2	-.08	-.12
14	Bolivia	150.3	-.15	-.15
26	Peru	154.6	-.12	-.15
1	Guatemala	171.2	-.29	-.10
22	Mexico	194.5	-.34	-.02
29	Mexico	194.4	-.79	-.39
21	Alaska	320.1	-.34	-.16
25	Alaska	313.2	-.58	-.25

RESIDUALS FOR CNK RELATIVE TO TCK AND THE MEAN

EVENT NUMBER	LOCALITY	AZIMUTH (deg)	RESIDUAL RELATIVE TO TCK (sec)	RESIDUAL RELATIVE TO MEAN (sec)
4	Chile	154.3	.43	-.03
10	Argentina	148.0	.31	.29
13	Bolivia	148.1	.42	.31
25	Peru	152.1	.16	.13
26	Peru	152.2	.26	.21
36	Peru	150.1	.35	.23
14	El Salvador	162.6	.72	.64
11	Mexico	177.3	-.48	-.15
16	Mexico	193.2	-.37	-.23
17	Mexico	169.3	-.36	-.06
21	Mexico	188.0	-.24	.08
28	Mexico	187.2	-.38	.02
32	Mexico	172.2	.48	.69
2	Alaska	325.1	-.30	-.15
20	Alaska	319.9	.04	.22
22	Alaska	312.0	-.16	.02
27	Alaska	323.8	-.08	.01
29	Alaska	322.7	.04	.08
23	California	282.5	-.12	.10

RESIDUALS FOR BEK RELATIVE TO TCK AND THE MEAN

EVENT NUMBER	LOCALITY	AZIMUTH (deg)	RESIDUAL RELATIVE TO TCK (sec)	RESIDUAL RELATIVE TO MEAN (sec)
15	Peru	153.8	.04	.01
1	Guatemala	169.0	-.04	.10
3	Nicaragua	159.9	-.09	.11
5	Costa Rica	158.4	-.08	.12
7	Mexico	196.1	-.27	-.23
17	Mexico	173.3	-.64	-.35
32	Mexico	176.0	-.13	.09

RESIDUALS FOR SNK RELATIVE TO TCK AND THE MEAN

EVENT NUMBER	LOCALITY	AZIMUTH (deg)	RESIDUAL RELATIVE TO TCK (sec)	RESIDUAL RELATIVE TO MEAN (sec)
4	Chile	154.3	.99	.54
10	Argentina	148.0	.20	.17
13	Bolivia	148.1	.42	.31
18	Colombia	152.1	.08	.06
25	Peru	152.1	.13	.08
26	Peru	138.9	.52	.47
14	El Salvador	162.5	.17	.09
6	Mexico	170.2	.32	.41
11	Mexico	177.5	-.16	.16
28	Mexico	188.7	-.28	.12
31	Mexico	170.3	-.17	-.04
32	Mexico	172.3	-.18	.40
2	Alaska	325.5	-.16	-.01
19	Alaska	312.1	.28	.21
20	Alaska	320.3	-.23	-.05
22	Alaska	312.4	-.29	-.12
24	Alaska	313.1	-.75	-.42
27	Alaska	324.2	-.27	-.19
33	Alaska	325.4	-.35	-.08
35	Alaska	311.2	-.60	.41
23	California	283.9	-.38	-.16

RESIDUALS FOR EMK RELATIVE TO TCK AND THE MEAN

EVENT NUMBER	LOCALITY	AZIMUTH (deg)	RESIDUAL RELATIVE TO TCK (sec)	RESIDUAL RELATIVE TO MEAN (sec)
4	Chile	155.3	.34	-.06
10	Argentina	149.1	.29	.25
13	Bolivia	149.2	.30	.30
25	Peru	153.3	.40	.38
25	Peru	153.3	.40	.34
5	Costa Rica	157.6	-.12	.01
30	Nicaragua	158.7	.63	.35
6	Mexico	173.3	-.29	-.16
7	Mexico	196.3	-.03	.06
8	Mexico	199.4	-.36	.01
9	Mexico	199.6	-.21	.08
11	Mexico	180.7	-.55	-.18
12	Mexico	180.8	-.45	.12
17	Mexico	172.8	-.42	-.08
21	Mexico	192.0	-.65	-.33
28	Mexico	191.6	-.79	-.39
31	Mexico	173.2	-.30	-.12
32	Mexico	175.5	-.37	-.10
20	Alaska	320.6	-.22	-.04
22	Alaska	312.9	-.26	-.09
24	Alaska	313.6	-.57	-.24
29	Alaska	323.2	-.17	-.13
23	California	285.3	-.30	-.09

RESIDUALS FOR MLK RELATIVE TO TCK AND THE MEAN

EVENT NUMBER	LOCALITY	AZIMUTH (deg)	RESIDUAL RELATIVE TO TCK (sec)	RESIDUAL RELATIVE TO MEAN (sec)
10	Argentina	148.7	-.04	-.02
13	Bolivia	148.8	.01	-.02
15	Peru	153.0	-.10	-.03
18	Colombia	140.0	.06	-.01
25	Peru	152.8	.001	-.02
26	Peru	152.9	.002	-.05
36	Peru	150.9	-.02	-.10
1	Guatemala	167.4	-.33	-.14
3	Nicaragua	158.5	-.33	-.13
5	Costa Rica	157.0	-.34	-.21
30	Nicaragua	158.7	.25	-.02
34	Nicaragua	158.0	-.37	.06
6	Mexico	172.0	-.47	-.33
7	Mexico	194.4	-.18	-.08
16	Mexico	195.5	-.08	.10
21	Mexico	190.2	-.10	.22
28	Mexico	189.7	.06	.46
31	Mexico	172.0	-.15	.03
2	Alaska	325.3	.17	.38
19	Alaska	312.2	.20	.17
20	Alaska	320.2	-.02	.16
22	Alaska	312.4	.08	.25
27	Alaska	323.9	.07	.16
29	Alaska	322.8	.05	.09
33	Alaska	325.1	-.12	.19
37	Alaska	313.6	.08	.13
23	California	283.6	.22	.44

RESIDUALS FOR HWK RELATIVE TO TCK AND THE MEAN

EVENT NUMBER	LOCALITY	AZIMUTH (deg)	RESIDUAL RELATIVE TO TCK (sec)	RESIDUAL RELATIVE TO MEAN (sec)
10	Argentina	150.1	-.45	-.54
13	Bolivia	150.2	-.67	-.71
18	Colombia	142.5	-.17	-.27
25	Peru	154.5	-.36	-.39
26	Peru	154.5	-.56	-.61
3	Nicaragua	161.7	-.38	-.18
14	El Salvador	167.4	-.55	-.64
34	Nicaragua	161.8	-.61	-.33
7	Mexico	197.4	.17	.21
8	Mexico	200.2	-.66	-.34
9	Mexico	200.4	-.55	-.31
11	Mexico	182.6	-.48	-.16
12	Mexico	182.7	-.22	-.65
17	Mexico	175.2	-.09	.20
21	Mexico	193.4	-.60	-.28
28	Mexico	193.1	-.44	-.04
32	Mexico	177.8	-.49	-.27
2	Alaska	324.6	-.52	-.37
19	Alaska	312.2	-.24	-.31
20	Alaska	319.6	-.41	-.22
22	Alaska	312.0	-.41	-.24
24	Alaska	312.6	-.34	-.01
27	Alaska	323.2	-.15	-.06
29	Alaska	321.9	-.38	-.34
33	Alaska	324.5	-.64	-.38
35	Alaska	311.4	-.15	-.28
37	Alaska	313.8	-.24	-.18
23	California	282.2	-.43	-.22

'RESIDUALS FOR TCK RELATIVE TO THE MEAN

EVENT NUMBER	LOCALITY	AZIMUTH (deg)	RESIDUAL RELATIVE TO MEAN (sec)
4	Chile	155.1	-.45
10	Argentina	148.9	-.03
13	Bolivia	149.0	-.05
15	Peru	153.2	-.03
18	Colombia	140.4	-.19
25	Peru	153.1	-.02
26	Peru	153.1	-.05
36	Peru	151.2	-.13
1	Guatemala	167.9	.14
3	Nicaragua	159.0	.20
5	Costa Rica	157.5	.08
14	El Salvador	164.6	-.08
30	Nicaragua	158.5	-.33
34	Nicaragua	159.2	.27
6	Mexico	172.5	.09
7	Mexico	194.6	.04
8	Mexico	197.9	.32
9	Mexico	198.0	.24
11	Mexico	179.7	.32
12	Mexico	179.8	.52
16	Mexico	195.8	.13
17	Mexico	172.0	.29
21	Mexico	190.5	.32
28	Mexico	190.0	.40
31	Mexico	172.5	.13
32	Mexico	174.7	-.62
2	Alaska	325.1	.15
19	Alaska	312.1	-.07
20	Alaska	320.0	.18
22	Alaska	312.2	.17
24	Alaska	312.8	.33
27	Alaska	323.7	.08
29	Alaska	322.5	.04
33	Alaska	324.9	.27
35	Alaska	311.2	-.13
37	Alaska	313.6	.06
23	California	283.0	.22

BIBLIOGRAPHY

Aki, Keiiti, Scattering of P-waves under the Montana Lasa, J. Geophys. R., vol. 78, pp. 1334-1346, 1973.

Anderson, D.L., Chemical plumes in the mantle, Geol. Soc. Am. Bull., vol. 86, pp.1593-1600, 1975.

Barr, K.G., and G.R. Robson, Seismic delays in the eastern Caribbean, Geophys. J., vol. 7, pp.342-349, 1963.

Bolt, B.A., and O.W. Nuttli, P-wave residuals as a function of azimuth, 1, Observations, J. Geophys. Res., vol. 71, pp. 5977-5986, 1966.

Bott, M.H.P., Formation of oceanic redges, Nature, vol. 207, pp. 840-843, 1965.

Cann, J.R., Geological processes at the midocean ridge crests, Geophys. J., vol. 5, pp. 331-341, 1968.

Chase, C., and T. Gilmer, Precambrian plate tectonics: The mid-continent gravity High: Earth and Planetary Sci. Let., vol. 21, pp. 70-78, 1973.

Chinnery, M.A., and, M.N. Toksoz, P-wave velocities in the mantle, 1, Below 700 km, Bull. Seismol. Soc. Amer., vol. 57, pp. 199-226, 1967.

Cleary, J., and A.L. Hales, An analysis of the travel times of P-waves to North American stations, in the distance range 32° to 100°, Bull. Seismol. Soc. Amer., vol. 56, pp.467-489, 1966.

Coe, Max, Computer locations of microearthquakes in Kansas, unpublished M.S. Thesis, University of Kansas, 1980.

Cole, V.B., Configuration of the top of the Precambrian rocks in Kansas, Kansas Geological Survey, Lawrence, Kansas, Map M-7, 1976.

Coons, R.L., G.P. Woolward, and G. Hershey, Structural significance and analysis of mid-continent gravity high, AAPG Bull., vol.51, pp.2381-2399, 1967.

Deffeyes, K.S., Plume convection with an upper-mantle temperature inversion, Nature, vol. 240, pp. 539-544, 1972.

Engdahl, E.R., J.G. Sindorf, and R.A. Eppley, Interpretation of relative teleseismic P wave Residuals, J. Geophys. Res., vol. 82, pp. 5671-5682, 1977.

Evans, J.R., and H.M. Iyer, Deep, low-velocity anomaly under the Yellowstone caldera, Seismol. Soc. Amer., Abs., Los Angeles, Ca., 1975.

Green, R.W.E., and A.L. Hales, The travel times of P-waves to 30° in the central United States and upper mantle structure, Bull. Seismol. Soc. Amer., vol. 58, pp. 267-289, 1968.

Gutenberg, B., Travel times of longitudinal waves from surface foci, Proc. Natl. Acad. Sci. U.S., vol. 39, pp. 849-853, 1953.

Hart, P.J., ed., The Earth's Crust and Upper Mantle, American Geophysical Union, Washington, D.C., 1969.

Health Sciences Computing Facility, University of California, Los Angeles, Program BMDP3R, 1979.

Herrin, E., Introduction to 1968 seismological tables for P-phases, Bull Seismol. Soc. Amer., vol. 58, p. 1193, 1968.

Herrin, E., and J. Taggart, Regional variations in Pn velocity and their effect on the location fo epicenters, Bull. Seismol. Soc. Amer., vol. 52, pp. 1037-1046, 1962.

Ibrahim, A.W.W., Areal Pn and Pg velocity variation in central United States, unpublished M.S. thesis, University of Kansas, 1963.

Iyer, J.M., Anomalous delays of teleseismic P-waves in Yellowstone National Park, Nature, vol. 253, pp. 425-427, 1975.

Iyer, H.M., and J.H. Healy, Teleseismic residuals at the Lasa--USGS extended array and their interpretation in terms of crust and upper mantle structure, J. Geophys. Res., vol. 77, pp. 1503-1527, 1972.

Iyer, H.M., D.H. Oppenheimer, T. Hitchcock, Abnormal P-wave delays in The Geysers--Clear Lake geothermal area, California, Science, vol. 204, pp. 495-497, 1979.

King, E., and I. Zeitz, Aeromagnetic study of the midcontinent gravity high of the central United States: GSA Bull., vol. 82, pp. 2187-2208, 1971.

Lidiak, E.G., Rifting in the midcontinent, U.S.A., (abst.) 1978 International Symposium on the Rio Grande Rift, Santa Fe, New Mexico, October 8-17, 1978.

Lui, C.Y., untitled, unpublished M.S. thesis, University of Kansas, 1980.

Mack, H., Nature of short-period P-wave signal variations at LASA, J. Geophys. Res., vol. 74, pp. 3161-3170, 1969.

Mueller, S., and M. Landisman, Seismic studies of the earth's crust in continents,, I: Evidence for a low-velocity zone in the upper part of the lithosphere, Geophys. J.R. astr. Soc., vol. 10, pp. 525-538, 1966.

Murase, T., and A.R. McBirney, Properties of some common igneous rocks and their melts at high temperatures, Geol. Soc. Amer. Bull., vol. 84, pp. 3563-3592, 1973.

Naizi, M., and D.L. Anderson, Upper mantle structure of western North America from apparent velocities of P-waves, J. Geophys. Res., vol. 72, pp. 4633-4648, 1965.

Nuttli, O.W., and B.A. Bolt, P-wave residuals as a function of azimuth, 2, Undulations of the mantle low-velocity layer as an explanation, J. Geophys. Res., vol. 74, pp. 6594-6602, 1969.

Ocola, L.C., and R.P. Meyer, Central North American rift system: 1. Structure of the axial zone from seismic and gravimetric data, J. Geophys. Res., vol. 78, pp. 5173-5194, 1973.

Press, F., and S. Beihler, Inferences on crustal velocities and densities from P-wave delays and gravity anomalies, J. Geophys. Res., vol. 69, pp. 2979-2995, 1964.

Reasenberg, P., Program ARRAY: An interactive seismic array processing program for use with data sets established by program EVCON, U.S. Geol. Survey Open-file Report 78-201, 1978.

Reasenberg, P., W. Ellsworth, and A. Walter, Teleseismic evidence for a low-velocity body under the coso geothermal area, (in press).

Richter, C.F., Elementary seismology, W.H. Freeman and Co., San Francisco, Ca., 1958.

Sipkin, S.A., and T.H. Jordan, Lateral heterogeneity of the upper mantle determined from the travel times of ScS, J. Geophys. Res., vol. 80, pp. 1474-1489, 1975.

Steeples, D.W., Teleseismic P-delays in geothermal exploration, with application to Long Valley, California [Ph.D. thesis]: Stanford, California, Stanford University, 1975.

----------, Preliminary crustal model for Northwest Kansas (abstract), EOS Trans. AGU, vol. 57, no. 12, p. 961, 1976.

Steeples, D.W., and H.M. Iyer, Low velocity zone under Long Valley as determined from teleseismic events, J. Geophys. Res., vol. 81, pp. 849-860, 1976.

Steeples, D.W., and H.M. Iyer, Teleseismic P-wave delays in geothermal exploration, Proceedings: Second United Nations Symposium on the development and use of geothermal resources, San Francisco, CA., vol. 2, pp. 1199-1206, 20-29, May, 1976.

Talwani, M., X. Le Pichon, and J.R. Heirtzler, East Pacific rise: The magnetic pattern and the fracture zones, Science, vol. 150, pp. 1109-1115, 1965.

Talwani, M., and G.H. Sutton, Comment on "Seismic delays in the eastern Carribbean" by K.G. Barr and G.R. Robson, Geophys. J., vol. 8, pp. 463-466, 1964.

Vogt, P.R., E.D. Schneider, and G.L. Johnson, The crust and upper mantle beneath the sea, in: The Earth's crust and upper mantle, American Geophysical Union, Washington, D.C., pp. 556-617, 1969.

Ward, J.R., Geohydrology of Nemaha County, Northeast Kansas: University of Kansas Publication, Groundwater Series No. 2, 1974.

Yarger, H.L., K. Ng, R. Robertson, and R. Woods, Bouguer gravity map of Northeastern Kansas, Kansas Geological Survey, Lawrence, Kansas, 1980.

Yarger, H.L., Aeromagnetic analysis of the Keweenawan rift in Kansas (abstract), AGU Midwest Meeting, Dekalb, Ill., 1980.